The role of the EGFR and ERBB4 in acute pancreatitis

von Franziska Stumpf

Inaugural-Dissertation

zur Erlangung der Doktorwürde

der Tierärztlichen Fakultät

der Ludwig-Maximilians-Universität München

The role of the EGFR and ERBB4 in acute pancreatitis

von Franziska Stumpf

aus München

München 2015

Aus dem Veterinärwissenschaftlichen Department

der Tierärztlichen Fakultät

der Ludwig-Maximilians-Universität München

Lehrstuhl für molekulare Tierzucht und Biotechnologie

Arbeit angefertigt unter der Leitung von

PD Dr. Marlon R. Schneider

Mitbetreuung durch: Dr. Maik Dahlhoff

Gedruckt mit der Genehmigung der Tierärztlichen Fakultät

der Ludwig-Maximilians-Universität München

Dekan: Univ.-Prof. Dr. Joachim Braun

Berichterstatter: PD Dr. Marlon R. Schneider

Korreferent: Univ.-Prof. Dr. Dušan Palić

Tag der Promotion: 18.Juli 2015

für Leopold

Der Mensch hat nicht das Recht über Tiere zu urteilen,
sie stammen aus einer anderen Welt,
die älter und vollständiger war als unsere jetzt,
ihre Erscheinung ist besser und vollständiger,
sie haben Eigenschaften,
die wir verloren oder nie erreicht haben…
sie sind keine Untertanen,
sie gehören einer anderen Nation an
-und sind nur durch Zufall mit uns zugleich
ins Netz der Zeit gefallen, die wir Glanz
und Plage zugleich für die Erde sind.

Beston Henry

INDEX

ABBREVATIONS

µg	microgram
µl	microliter
µm	micrometer
µM	micromole
A	ampere
ADAM	a disintegrin and metalloproteinease
AKT	protein Kinase B
AREG	amphiregulin
AZ	Aktenzeichen
BCA	bicinchoninic acid
bp	base pairs
BrdU	bromodeoxyuridine
BSA	bovine serum albumin
BTC	betacellulin
Cbg/CBG	Corticosteroid-binding globulin
cDNA	complementary deoxyribonucleic acid
cm	centimeter
cm^2	square centimeter
CMV	cytomegalovirus
Co	control
Cre	causes recombination
$CuSO_4$	cupric sulphate
CYT	cytosolic
d	day
DEPC	diethylpyrocarbonate
DIG	digoxigenin
dl	deciliter
DNA	deoxyribonucleic acid
dNTPs	deoxynucleotides
e.g.	*exempli gratia*
E9.5	embryonic day 9.5
EDTA	ethylenediaminetetraacetic acid

EGF	epidermal growth factor
EGFR	epidermal growth factor receptor
EPGN	epigen
ERBB	avian erythroblastosis oncogene B homologue
EREG	epiregulin
FBS	fetal bovine serum
Fig.	figure
g	gram
Gapdh	glyceraldehydes-3-phosphate dehydrogenase
h	hour
H&E	hematoxilin and eosin
HBEGF	heparin-binding-EGF-like growth factor
HCl	hydrochloric acid
HER	human epidermal growth factor receptor
H_2O	water
H_2O_2	hydrogen peroxide
HPF	high power field
ICD	intracellular domain
JM	juxtamembrane
kb	kilobase
KCl	potassium chloride
kDa	kilo dalton
kg	kilogram
KH_2PO_4	monopotassium phosphate
KO	knockout
l	liter
loxP	locus of crossing-over
M	molar
mA	milliampere
mg	milligram
$MgCl_2$	magnesium chloride
min	minute
ml	milliliter
mm	millimeter
mM	millimolar

Mmp2	matrix metalloproteinase-2
Mmp3	matrix metalloproteinase-3
mRNA	messenger ribonucleic acid
Na_2HPO_4	sodium dihydrogen phosphate
NaCl	sodium chloride
NaOH	sodium hydroxide
ng	nanogram
nm	nanometer
nmol	nanomole
NRG	neuregulin
PAGE	polyacrylamide gel electrophoresis
PBS	phosphate buffered saline
PCR	polymerase chain reaction
Pedf/PEDF	Pigment epithelium-derived factor
RIP	regulated intramembrane proteolysis
RNA	ribonucleic acid
rpm	revolutions per minute
RT-PCR	reverse transcriptase polymerase chain reaction
RTK	receptor tyrosine kinase
RV	reverse
s	second
SAPK	stress activated protein kinase
SDS	sodium dodecyl sulfate
serpina6	serine peptidase inhibitor, clade A, member 6
Serpinf1	serine peptidase inhibitor, clade F, member 1
TAE	tris-acetate-EDTA buffer
Taq	thermus aquaticus
TBS	tris buffered saline
TBST	tris buffered saline Tween20
TEMED	N,N,N',N'-tetraethylathylendiamine
tg	transgenic
TNF-α	tumor necrosis factor-alpha
Tris	tris-(hydroxymethyl)-aminomethane
U	unit
V	volt

Wa5	waved 5 (*Egfr*$^{+/Wa5}$ mouse)
wt	wildtype

I. INTRODUCTION

Different substances such as hormones, cytokines or growth factors play an important role during tissue homeostasis and in the regulation of most cellular functions. The classical hormones are transported by the blood system over long distances until they reach their target. Cytokines are expressed in nearly every tissue and have mostly a local effect. Growth factors have a position in between: They are expressed in almost every tissue and can also act over long distances. Some growth factors are expressed as membrane bound precursors on the cell surface and can interact with the extracellular domain of receptors like receptor tyrosine kinase (RTK). They can activate cell surface receptors to induce signal transduction cascades and thereby regulate gene expression, cell differentiation, cell metabolism, apoptosis and proliferation (Massague, 1993).

The Epidermal Growth Factor Receptor family is one of the most important receptor families and includes four receptors: ERBB1 (EGFR, HER1), ERBB2 (HER2, neu), ERBB3 (HER3) and ERBB4 (HER4). These receptors are expressed in several tissues and can regulate different physiological and pathological processes (Yarden, 2001), including cancer development (Pinkas-Kramarski, 1998). The ERBB receptors can be activated by eleven different ligands. These ligands can be receptor-specific or activate several receptors of the ERBB family (Holbro, 2003).

The ERBB receptors play a role in inflammation processes (Scheller, 2011) such as acute pancreatitis (AP), an inflammatory disease of the exocrine part of the pancreas. AP is characterized by acute abdominal pain in the epigastric area and increased serum levels of pancreatic enzymes such as amylase and lipase. Gallstone migration and alcohol consumption are the most common causes of acute pancreatitis. Fortunately, the mortality rate is lower than 5%. However, the risk to develop severe disease is about 20%. Organ failure associated with circulatory disorder in the early stage and infectious complications, such as infected pancreatic necrosis in the late stage are the main reasons for the mortality of pancreatitis patients (Matsumoto, 2014). AP seems to be caused by a regulation defect of trypsinogen, leading to cell death and the rise of pancreatic enzymes in the blood (Nemeth, 2013).

Betacellulin (BTC), a ligand of EGFR and ERBB4, has a protective effect against AP (Dahlhoff, 2010). ERBB4 is predominantly expressed in the exocrine part of the pancreas, and the EGFR in the endocrine pancreas. In this study we investigated whether the BTC-mediated protection against AP is mediated by EGFR or ERBB4.

II. REVIEW OF THE LITERATURE

1. The Epidermal Growth Factor Receptor family

All ERBB family members have an extracellular domain, followed by a single membrane-spanning region and a cytoplasmic domain (Olayioye, 2000). Receptor binding initiates dimerization of homo- and heterodimers and this formation leads to an autophosphorylation of specific tyrosine residues in the cytoplasmic domain. This process is followed by a complex cascade of downstream signalling pathways which are responsible for numerous effects affecting development, physiology, and pathology (Holbro, 2003), (Yarden, 2001). The ERBB2 receptor has no known ligand and the ERBB3 receptor does not contain an active tyrosine kinase (Linggi, 2006). Each receptor, with its unique signalling properties, can be specifically activated by its ligands (Beerli, 1996), (Sweeney, 2000). However, only the EGFR and the ERBB4 receptor can be activated as homodimer. Eleven different growth factors have the ability to bind and activate the ERBB receptors. Based on their binding specifity, the ligands can be divided into three groups: The first group includes epidermal growth factor (EGF) itself, transforming growth factor-α (TGFA), epigen (EPGN) and amphiregulin (AREG), which can activate only EGFR. The second group includes heparin-binding EGF-like growth factor (HBEGF), epiregulin (EREG), and betacellulin (BTC). These ligands have the skills to bind both the EGFR and the ERBB4 receptor. The neuregulins represent the third group. They can be divided into two subgroups based on their capacity to bind only ERBB4 or ERBB3 and ERBB4 (Holbro, 2003), (Harris, 2003). In addition, BTC and EGF can activate the ERBB2/ERBB3 heterodimer. The ERBB ligands are mainly synthesized as a transmembrane type I protein that can be cleaved by cell surface proteases to release the mature growth factor as a soluble form. All these ligands include a domain encompassing about 50 amino acids and possessing six characteristically spaced cysteines which form three intramolecular disulfide bonds leading to a three loop secondary structure. This sequence (called the EGF motif) is the precondition for ERBB receptor binding and activation (Harris, 2003),(Schneider, 2009).

The EGFR elicit manifold actions during development in adult mammals. HBEGF

is the only ligand whose absence results in postnatal lethality, due to malformed heart valves, hypertrophic cardiomyocytes, and hypoplastic lungs (Jackson, 2003) while mice lacking EGF (Luetteke, 1999), EREG ((Lee, 2004); (Shirasawa, 2004), AREG (Luetteke, 1999), BTC (Jackson, 2003), TGFA (Luetteke, 1993), and even triple null mice deficient for EGF, AREG and TGFA (Luetteke, 1999) are viable. These observations clearly signify that there is a high rate of redundancy within the family of EGFR ligands (Qin, 2005).

Signalling by activated ERBB receptors includes the following pathways: mitogen activated protein kinase (MAPK), phospholipase Cγ, signal transducer and activation of transcription (STAT), protein kinase B (PKB/AKT) and stress activated protein kinase (SAPK), which are common to nearly all RTKs. Activated ERBB receptors are processed from the cell surface by an endocytotic pathway resulting in rapid receptor degradation. Related to the intracellular migration of ERBB receptors, each of these receptors has been reported to be present in the nucleus. Relocalization of the EGFR and the ERBB4 receptor is a ligand-dependent process which can also influence gene expression and might represent a new signalling mechanism (Linggi, 2006).

2. ERBB4 expression and signalling

ERBB4, a glycoprotein of 180 kDa (Plowman, 1993), can be detected like all ERBB receptors in almost every tissue and is known to play an important role in the development of neuronal tissue, the heart and the mammary gland (Jones, 2003). The ERBB4 receptor has been also detected in neoplastic tissue like neoplastic thyroid, medulloblastoma, and neoplastic prostate (Srinivasan, 1998). Its role in the development of the pancreas, and in AP, is still unknown (Veikkolainen, 2012). The presumed role of ERBB4 in the development of the exocrine pancreas and AP in interaction with its ligand BTC, which protects mice against AP, is based on the finding that ERBB4 is predominantly expressed in the exocrine part of the pancreas (Dahlhoff, 2010),(Kritzik, 2000), (Huotari, 2002) and has been shown to have proapoptotic properties (Sartor, 2001), (Vidal, 2005), (Naresh, 2006).

The role of ERBB4 in other inflammation processes, described in multiple

publications, includes lung inflammation (Purevdorj, 2008) and Crohn's colitis, where ERBB4 is believed to promote cell survival and replacement after injury or inflammation (Frey, 2009).

The expression of ERBB4 starts at E9.5 (Gassmann, 1995). It is assumed that ERBB4 receptor signalling shows a number of characteristic features. The stress activated protein kinase (SAPK) pathway might be initiated by BTC via ERBB4 in AP, which seems to ensure a protective effect in AP due to an increased apoptosis induction (Dahlhoff, 2010). ERBB4 is expressed as alternatively spliced isoforms with different intracellular cytoplasmic (CYT) and extracellular juxtamembrane (JM) domains. By ligand activation the ERBB4 JM type a (JM-a) is cleaved and leads to a regulated intramembrane proteolysis (RIP) and an intracellular C-terminal domain is released (ICD) in the cytoplasm (Zeng, 2009). RIP was shown to be an alternative signalling pathway in ERBB4 signalling which leads to receptor proteolysis by TACE/ADAM17 and the release of the intracellular domain of ERBB4 in the cytoplasm (Rio, 2000), (Naresh, 2006). The disintegrin and metalloproteinase 17 (ADAM17), also called tumor necrosis factor-α converting enzyme (TACE), is a membrane-bound enzyme that cleaves ligands of ERBB receptors. The ectodomain shedding of these molecules can alter their biology and impact on immune and inflammatory responses and cancer development (Scheller, 2011). The 120 kDa ICD of ERBB4 can be either degraded through ubiquination or translocate to the nucleus to regulate gene expression and cell functions. Two ICD isoforms are known: CYT-1 and CYT-2. They differ at their cytoplasmic tails by including (CYT-1) or not (CYT-2) a 16-amino acid stretch containing binding sites for phosphoinositide 3-kinase (PI3-K) (Kainulainen, 2000) (Elenius, 1999) and the WW domain-containing e.g. Nedd-like ubiquitin ligases (Sundvall, 2008), (Zeng, 2009).

Unlike to the EGFR which is degraded efficiently through endocytosis, little is known about ERBB4 receptor degradation. It could be shown that ERBB4 cannot be degraded through endocytosis but by ubiquination, a process where ubiquitin is conjugated to side chains of proteins (Zeng, 2009).

3. Betacellulin

BTC was originally isolated from a mouse pancreatic β-tumor cell line as a 32-kDa glycosylated protein (Shing, 1993). BTC is able to activate EGFR, ERBB4 (Holbro, 2003) and all possible combinations of ERBB heterodimers, including the oncogenic ERBB2/3 heterodimer (Alimandi, 1997),(Pinkas-Kramarski, 1998). BTC can be found in almost every tissue and body fluids (Dunbar, 2000). Like other ERBB ligands, the expression of BTC can be upregulated upon receptor activation by BTC itself (auto-induction) or by other ERBB family members (cross-induction). This kind of regulation has been observed in rat intestinal epithelial cells, pancreatic cancer cell lines, human head and neck squamous carcinoma cells and human keratinocytes, suggesting an additional level of EGFR signal integration (Barnard, 1994),(Yokoyama, 1995),(Kawaguchi, 2000),(P, 2000).

In the mouse, the tissues with the highest endogenous BTC expression are the lung, the kidney, the uterus (Shing, 1993),(Ogata, 2005) and the pancreas, where BTC seems to play a role in islet regeneration (Li, 2001). BTC contains, like all ERBB ligands, the EGF motif and is synthesized as a transmembrane precursor. Proteolytic cleavage leads to the soluble and mature form of BTC. There is 74% identity between the human and the mouse BTC primary structure (Dunbar, 2000). BTC displays some unique properties at the structural and functional level. In addition to the EGF motif, additional cysteines are found that might form a fourth disulfide bridge. BTC features an Arg-Gly-Asp (RGD) sequence, presumed to influence cell-cell interactions. In addition, a disintegrin and metalloprotease 10 (ADAM10) was identified as the main shedding enzyme for BTC and EGF (Sahin, 2004).

Endogenous BTC induces the expansion of progenitor populations of neural stem cells and neuroblasts in the mouse brain (Gomez-Gaviro, 2012). This effect is mediated by both EGFR and ERBB4. Furthermore, BTC affects cell proliferation, differentiation, and survival, when added to cultured cell lines (Dunbar, 2000).

Mice lacking BTC expression are viable, fertile and show no overt defects (Jackson, 2003) in contrast to mice with ubiquitous BTC-overexpression (*Btc* transgenic mice) which show reduced body weight gain, a lung and eye pathology and also the pancreas weight is significantly reduced (Schneider, 2005). Acinar

apoptosis and proliferation is significantly increased in the pancreas of *Btc* transgenic animals. Moreover, the examination of the pancreas weight showed no difference between *Btc* transgenic mice and *Btc* transgenic mice with an additional hypomorphic mutation of the *Egfr* gene (*Btc+Wa5*). This observation indicates that the effects of BTC on the exocrine pancreas are EGFR-independent (Dahlhoff, 2010).

In addition, mice overexpressing ubiquitously BTC are protected against caerulein-induced and L-arginine-induced pancreatitis, showing significantly decreased amylase and lipase levels, reduced acinar necrosis, inflammation and edema in pancreatitis experiments. The analysis of signalling pathways indicated a dependence of the protective effect on JNK / SAPK (Dahlhoff, 2010).

4. Pancreas and acute pancreatitis

4.1. Exocrine pancreas

The pancreas is a retroperitoneal organ without a capsule. The pancreas contains a head, body, tail and the uncinate process. The second and third portion of the duodenum curves around the head of the pancreas. The pancreatic tail is adjacent to the spleen. The distal end of the common bile duct, which joins the pancreatic duct entering the duodenum, passes through the head of the pancreas. For this reason, pathologic processes of the pancreas can lead to biliary system obstruction and injury. There are also important relationships between the exocrine and the endocrine pancreas (islets of Langerhans). The blood from the endocrine pancreas flows directly in the capillaries of the exocrine tissue surrounding each of the islets before entering the general circulation. This special blood flow works as a kind of „portal“-system, protecting the surrounding tissue of the islets of high hormone concentrations (The exocrine pancreas, Stephen J.Pandol), (Untersuchungen über das Gefässystem des Pankreasläppchens bei verschiedenen Säugern mit besonderer Berücksichtigung der Kapillarknäuel der Langerhansschen Inseln, Annemarie Thiel, 1953).

The islets of Langerhans produce the following hormones: insulin (β-cells), amylin, glucagon (α-cells), somatostatin (δ-cells) and pancreatic polypeptide (PP-cells). The effect of these hormones on the exocrine pancreas is not known in

detail (Lazarow, 1957), (The exocrine pancreas, Stephen J.Pandol). The acinar cells for example have insulin receptors that are involved in the regulation of digestive enzyme synthesis. The functional unit of the exocrine pancreas consists of an acinus and its draining ductule. The acinus (from the Latin term meaning "berry in a cluster") contains specialized acinar cells which are able to synthesize, store, and secrete digestive enzymes. On the basolateral membrane, receptors for different hormones and neurotransmitters are located. Activating these receptors stimulate the secretion of the digestive enzymes. The apical region of the cell accumulates zymogen granules and enzymes. Additionally there are microvilli on the apical surface of the acinar cells. Those microvilli, together with the cytoplasm, work as a filamentous actin meshwork, which is involved in exocytosis of the contents of the zymogen granules. There are tight junctions between acinar cells to form a barrier and prevent the passage of large molecules, such as the digestive enzymes. The junctional complexes also permit the paracellular passage of water and ions (The exocrine pancreas, Stephen J.Pandol). The pancreatic acinus and the large ducts seem to develop polyclonally by multiple progenitor cells. They might result from an assembly of small ducts developing from a single origin (Ryu, 2013).

The ERBB receptors and their ligands are important for the development of the pancreas and the differentiation of the acinar cells. EGF for example is able to stimulate directly pancreas growth (Dembinski, 1982) and exocrine secretion (Konturek, 1984). It is also known that the ERBB receptors play a role in pancreatic adenocarcinoma and in chronic pancreatitis (te Velde, 2009) as well as in AP (Dahlhoff, 2010).

4.2. Acute Pancreatitis in humans and in animal models

AP is an inflammatory disease of the exocrine part of the pancreas. The yearly incidence of AP in the United States is approximately 32-44 new cases per 100000 population individuals and has increased over the last decade. This increase in incidence has been observed worldwide. AP is the most common cause of gastrointestinal related hospitalizations, with more than 274000 hospitalizations in 2012 (Tyler Stevens, 2009). AP is clinically manifested by abdominal pain and a concomitant rise in serum amylase and lipase. The most

common causes are alcohol abuse and gallstone migration. About 80% of the cases of AP run a benign course. Our knowledge about the pathology of AP is mainly based on animal studies. The inflammatory process starts in the acinar cells where zymogens and lysosomale granules are made fragile by substances such as alcohol and its metabolites. Substances released by the granules activate intracellular digestive enzymes, like trypsin (Vonlaufen, 2007). Because of the premature activation of these digestive enzymes the pancreatic tissue is autodigested, and leucocytes start to immigrate. Due to that autodigestion, the release of amylase and lipase in the blood can be detected as a biochemical marker for AP (Matull, 2006). The mortality rate is directly influences by the systemic inflammatory response syndrome (SIRS) (Schepers, 2013) and the infection of pancreatic necrosis (Muller, 2007).

To get a better insight into the course of AP, several animal models of AP have been developed, mostly in rodents. It is important to mention that not all aspects of the human disease can be reproduced in the experimental models. Nevertheless there are experimental models which can reveal some important aspects of AP in humans. Intraperitoneal injections of caerulein cause a mild, self-limiting form of AP in mice. This model can be used to study the activation of signalling pathways, synthesis of cytokines and the alteration of the cytoskeleton during AP (Schmid, 2005). Caerulein causes AP through activation of chymotrypsinogen, what leads to an auto activation of trypsinogen (Nemeth, 2013). After three intraperitoneal injections of 50 μg/kg body weight, caerulein leads to a threefold increase of serum amylase, and an increase of pancreatic body weight of 34%. The highest levels of serum amylase and pancreatic body weight can be observed 12 hours after starting the injections (Niederau, 1985). In the caerulein-induced pancreatitis the cell death is either initiated by necrosis or apoptosis. The severity of the pancreatitis correlates directly with the number of necrotic acinar cells and in inverse ratio with the number of apoptotic cells (Gukovskaya,2004).

III. ANIMALS, MATERIAL AND METHODS

1. Animals

All mice were bred and handled under specific pathogen free conditions in a closed barrier system at 22°C, 65% humidity and a 12 h light cycle in the Gene Center, LMU Munich. All animals received standard food (V1536; Ssniff, Soest, Germany) and water *ad libitum.* At the age of four weeks the mice were weaned, separated by gender, marked by ear clipping and housed in Makrolon cages type 2 or 3. At the same time tail tips for genotype analysis were taken and frozen by -80°C. If phenotype studies started earlier, foot tattooing was used to identify the animals. All animal experiments were carried out in accordance with the German Animal Protection Law with permission from the responsible veterinary authority (AZ 55.2-1-542531-138-10).

1.1. Conditional *Erbb4* knockout mice

Mice with a loss of function in the *Erbb4* gene in all tissues die in utero between day 10 and 11 after fertilization (E10-11) due to heart muscle developmental abnormalities (Gassmann, 1995). Therefore we generated conditional *Erbb4* knockout mice (*Erbb4-KO)* for the exocrine pancreas using the Cre-loxP-system. In *Ptf1a*$^{tm1(cre)Hnak}$ (*Ptf1a*-Cre) mice the *Cre* enzyme is expressed under the control of the pancreas-specific *Ptf1a* promoter (Nair, 2013), (Delaspre, 2013) *Ptf1a-Cre* mice were mated with *B6;129-Erbb4*^{tm1Fej}*/Mmucd* (*Erbb4*$^{fl/fl}$) mice to delete the loxP-flanked exon 2 of the *Erbb4* gene. The resulting mRNA of the *Erbb4* gene carries a frame shift. The *Ptf1a* $^{tm1(cre)Hnak}$ mice were kindly provided by Hana Algül, PD Dr. med (Klinikum rechts der Isar, Munich). The resulting *Erbb4-KO* mice stay alive and show no overt differences during their development compared to their wildtype littermates.

1.2. Egfr$^{+/Wa5}$ mice

Egfr$^{+/Wa5}$ (*Wa5*) mice were generated by a N-ethyl-N-nitrosourea (ENU) mutagenesis program and are maintained in the C57BL/6N background (Lee, 2004). These mice carry a mutation altering the highly conserved DFG motif within the activation loop of the *Egfr* kinase domain. This point mutation results in the expression of a dominant negative EGF-receptor. Homozygous embryos die during gestation while heterozygous *Egfr*$^{+/Wa5}$ survive. They have opened eyes at birth, a wavy coat and an abnormal placental constitution. *Wa5* mice are an accepted EGFR in vivo knockdown model as less than 10 % of the EGFR activity is maintained.

1.3. *Btc* transgenic mice

For our experiments we used the ubiquitous BTC-overexpressing mice pTORU-Btc (Schneider, 2005). This transgenic mouse line was established by pronuclear DNA microinjection into zygotes. The mice show the highest BTC expression levels in the heart, lung, brain, and the pancreas. They exhibit high early postnatal mortality, reduced body weight gain, and impaired longitudinal growth. Cataract and abnormally shaped retinal layers as well as bone alterations leading to a dome-shaped, round head form were also observed in *Btc* transgenic mice. The reduced life expectancy is related to several alterations of the lung e.g. alveolar hemorrhage and thickening of the alveolar septa. *Btc* transgenic mice show also significantly reduced pancreas weight compared to their wildtype littermates (Schneider, 2005).

1.4. Gt (ROSA)26Sor$^{tm/Sor}$ mice

Mice homozygous for the ROSA26 retroviral insertion display no distinguishing phenotype. LacZ is expressed in all tissues of the developing embryo and in most tissues of the adults. Crossbreeding with *Gt (ROSA)26Sor*$^{tm/Sor}$ reporter mice reveals in which tissue the Cre enzyme is expressed. The transgene consists of a floxed neomycin cassette followed by four polyA sequences and the reporter gene lacZ (Soriano, 1999). In the presence of the Cre recombinase the floxed sequence is deleted and the LacZ sequence can be transcribed.

1.5. Breeding strategy

To obtain *Btc* transgenic mice in the *Egfr* knockdown background, pTORU-Btc mice were mated with *Wa5* mice, resulting in following genotypes: controls (*Egfr*$^{+/+}$), *Wa5* (*Egfr*$^{+/Wa5}$), pTORU-Btc (*Btc*; *Egfr*$^{+/+}$) and *Btc*+*Wa5* (*Egfr*$^{+/Wa5}$; *Btc*). To obtain *Btc* transgenic mice in the *Erbb4* knockout background, pTORU-Btc were mated with *Erbb4-KO* mice, resulting in following genotypes: Controls (Erbb4$^{fl/fl}$, Erbb4$^{fl/+}$, Erbb4$^{fl/+}$;*Ptf1a*-Cre, and Erbb4$^{+/+}$;*Ptf1a*-Cre), *Erbb4-KO* (Erbb4$^{fl/fl}$;*Ptf1a*-Cre),pTORU-Btc (*Btc*;Erbb4$^{fl/+}$,Btc;Erbb4$^{+/+}$, *Btc*;Erbb4$^{fl/+}$;*Ptf1a*-Cre, and Btc;Erbb4$^{+/+}$;*Ptf1a*-Cre) and *Btc*+*Erbb4-KO* (Erbb4fl/fl;*Ptf1a*-Cre;*Btc*).

2. Principle of the Polymerase Chain Reaction (PCR)

With this *in vitro* method it is possible to multiplicate a selected DNA sequence millions of times. The oligonucleotide primers hybridize to two opposite DNA strands to flank the sequence of interest. The combination of deoxyribonucleoside triphosphates (dNTPs) and a heat-stable DNA polymerase catalyzes the elongation of the primers. In each cycle the template is denaturized, and the annealed primers are extended by the polymerase. The DNA-polymerase is an enzyme that completes single-strand DNA to a double-strand molecule. The double-strand DNA is again denaturized in the next cycle and the number of templates rises exponentially corresponding to each cycle. Each primer has its own annealing temperature, the temperature that allows them to specifically hybridize to the DNA strand.

2.1. PCR protocol for detecting *Btc* transgenic mice

Taq DNA polymerase Kit (Qiagen) containing:

PCR Buffer, 10 x	Tris-HCl, KCl, $(NH_4)SO_2$, 15mM $MgCl_2$, pH 8.7 (20°C)
Q-Solution	5x concentrated
MgCl	25mM
Taq Polymerase	5 U/µl, recombinant 94-kDa DNA polymerase, isolated from *Thermus aquaticus*, cloned in E.coli
dNTPs Set	100 mM aqueous solutions of dATP, dCTP, dGTP and dTTp, each in a separated vial

Reagents for separating the PCR products in agarose gel and visualizing under UV light:

Ethidium bromide	0.1% solution in bidistilled H_2O
50x TAE running buffer	242 g TRIS 57.1 ml Glacial Acetic Acid 100 ml EDTA, 0.5M , pH 8.0 Ad 1 l bidistilled H_2O
6x Loading Dye	30% glycerol bromophenol blue

To confirm that the *Btc* construct was integrated the following primers were used:

pTORUseq	5'-CTACAGCTCCTGGGCAACGTG-3'
globpA	5'-AGATCTCAGTGGTATTTGTGAGCC 3'

Assay procedure

We used 100 µl PCR tubes to prepare a 20 µl reaction. The PCR tubes were stored on ice during the whole preparation time.

DNA template (about 50 ng)	1 µl
Sense primer (2 µM)	1 µl
Antisense primer (2 µM)	1 µl
dNTPs Mix (1mM)	2 µl
PCR Buffer, 10x	2 µl
Q-solution	4 µl
$MgCl_2$ (25mM)	1.25 µl
Taq Polymerase (5U/µl)	0.1 µl
Bidistilled H_2O	7.65 µl

For the amplification, a Biometra Uno Thermocycler (Göttingen, Germany) was used with the following program:

1st step:	Denaturation	94°C for 4 min
2nd step:	Denaturation	94°C for 1 min
3rd step:	Annealing	60°C for 1 min
4th step:	Extension	72°C for 2 min
5th step:	Extension	72°C for 10 min
5th step:	Cooling	4°C

Steps 2 to 4 were repeated 35 times before progressing to step 5 and 6 (36 cycles). PCR products were separated in a 1.5 % agarose TAE gel with ethidium bromide and visualized under UV light.

2.2. PCR protocol for detecting the mutated *Egfr* sequence

Taq DNA polymerase Kit (Qiagen) was used as described above.

To detect the *Wa5* sequence the following primers were used:

Wa5As1	5'-TAGAGAATGACCCTGACGAG-3'
Wa5S6	5'-GCATGTCAAGATCACAGG-3'

The product has a total length of 228 bp.

Assay procedure

For the amplification the following protocol was used:

1st step:	Denaturation	94°C for 4 min
2nd step:	Denaturation	94°C for 30 sec
3rd step:	Annealing	58°C for 20 sec
4th step:	Extension	72°C for 2 min
5th step:	Extension	72°C for 8 min
5th step:	Cooling	4°C

Steps 2 to 4 were repeated 37 times before progressing to step 5 and 6 (38 cycles). PCR products were separated in a 1.5 % agarose TAE gel with ethidium bromide and visualized under UV light.

2.3. PCR protocol for detecting the sequence for the Cre enzyme

Taq DNA polymerase Kit (Qiagen) was used as described above.

To detect the *Cre* sequence we used the following primers:

Cre-1	5'-AATCGCCATCTTCCAGCAGG-3'
Cre-2	5'-GATCGCTGCCAGGATATACG-3'

Assay procedure

For the amplification the following protocol was used:

1st step:	Denaturation	94°C for 4 min
2nd step:	Denaturation	94°C for 1 min
3rd step:	Annealing	58°C for 2 min
4th step:	Extension	72°C for 1 min
5th step:	Extension	72°C for 4 min
5th step:	Cooling	4°C

Steps 2 to 4 were repeated 35 times before progressing to step 5 and 6 (36 cycles). PCR products were separated in a 1.5 % agarose TAE gel with ethidium bromide and visualized under UV light.

2.4. PCR protocol for detecting the floxed *Erbb4* sequence

Taq DNA polymerase Kit (Qiagen) was used as described above

To detect the floxed exon 2 of the *Erbb4* gene the following primers were used:

P20	5'-CAAATGCTCTCTCTGTTCTTTGTGTCTG-3'
P22	5'-TTTTGCCAAGTTCTAATTCCATCAGAAGC-3'

The product has a total length of 400 bp.

To detect the wildtype allele we used:

P20	5'-CAAATGCTCTCTCTGTTCTTTGTGTCTG-3'
P23	5'-TATTGTGTTCATCTATCATTGCAACCC-3'

The product has total length of 350 bp.

Assay procedure

DNA template (about 50 ng)	1 µl
Sense primer (20 µM)	1 µl
Antisense primer mutant (20 µM)	1 µl
Antisense primer wildtype (20 µM)	1 µl
dNTPs Mix (1mM)	2 µl
PCR Buffer, 10x	2 µl
Q-solution	4 µl
$MgCl_2$ (25mM)	1.25 µl
Taq Polymerase (5U/µl)	0.1 µl
Bidistilled H_2O	6.65 µl

For the amplification the following protocol was used:

1st step:	Denaturation	94°C for 2 min
2nd step:	Denaturation	94°C for 1 min
3rd step:	Annealing	58°C for 2 min
4th step:	Extension	72°C for 2 min
5th step:	Extension	72°C for 1 min
5th step:	Cooling	4°C

Steps 2 to 4 were repeated 35 times before progressing to step 5 and 6 (36 cycles). PCR products were separated in a 1.5 % agarose TAE gel with ethidium bromide and visualized under UV light.

2.5. PCR protocol for detecting the modified *LacZ* gene driven by the cell type-independent *ROSA26* promoter

Taq DNA polymerase Kit (Qiagen) was used as described above.

To detect the modified *LacZ* gene the following primers were used:

r26 RGT 1	5'-AAAGTCGCTCTGAGTTGTTAT-3'
r26 RGT 2	5'-GCGAAGAGTTTGTCCTCAACC-3'
r26 RGT 3	5'-GGAGCGGGAGAAATGGATATG-3'

Assay procedure

DNA template (about 50 ng)	1 µl
Sense primer	1 µl
Antisense primer	1 µl
Antisense primer 2	1 µl
dNTPs Mix (1mM)	2 µl
PCR Buffer, 10x	2 µl
Q-solution	4 µl
$MgCl_2$ (25mM)	1.25 µl
Taq Polymerase (5U/µl)	0.1 µl
Bidistilled H_2O	6.65 µl

For the amplification the following protocol was used:

1st step:	Denaturation	94°C for 5 min
2nd step:	Denaturation	94°C for 1 min
3rd step:	Annealing	58°C for 1 min
4th step:	Extension	72°C for 2 min
5th step:	Extension	72°C for 10 min
5th step:	Cooling	4°C

Steps 2 to 4 were repeated 35 times before progressing to step 5 and 6 (36 cycles). PCR products were separated in a 1.5 % agarose TAE gel with ethidium bromid and visualized under UV light.

3. Evaluation of gene expression at RNA level

3.1. Extraction of RNA from tissue

To isolate RNA from tissue, all working solutions were treated with 0.01% DEPC (diethylpyrocarbonat) to inhibit ribonucleases. The treated solutions were left at room temperature overnight and autoclaved the other day. In addition, only RNase-free pipette tips and gloves were used. After the mice were killed by cervical dislocation, the organs were extracted carefully and three samples of different regions of the pancreas were immediately put into 100 µl ice-cold TRIzol® (Invitrogen, Germany) and homogenized with a tissue homogenizer (Miccra, Germany) for 30 sec and stored on ice. Between two samples the homogenizer was cleaned with bidistilled water and 0.2 M NaOH. Before the RNA isolation samples were left at room temperature for 5 minutes. In the next step 200 µl chloroform were added and vortexed to mix the reagents. The samples were left for 10 min at room temperature. Then all samples were centrifuged at 12000x g for 15 min at 4°C. The upper aqueous phase of the supernatant was pipetted into a new RNase-free centrifuge tube. 500 µl isopropanol and 50 µl 3M sodium acetate were added, mixed by inverting, and the tube was left for 10 minutes at room temperature. Subsequently the tubes were centrifuged at 12000x g for another 10 min at 4°C. The pellets were washed twice with 900 µl 75% ethanol, vortexed and centrifuged at 12000x g for 5 minutes at 4°C. The supernatant was discarded to dry the pellets for 5 to 10 min. After that the pellet was dissolved in 50 µl DEPC treated bidistilled water and left for 10 minutes at 55°C. We determined the final RNA concentration with the NanoDrop® spectrometer ND-1000 (260 nm). The quality of the RNA was confirmed by electrophoresis using a 1% agarose gel, stained with ethidium bromide. The 18S and 28S RNA bands were visualized under UV light. The isolated RNA was stored at -20°C.

3.2. cDNA synthesis

1 ng RNA was dissolved in DEPC-water to a total volume of 8.5 µl. For the transcription the Thermo kit was used according to the manufacture's introduction. Each sample was mixed with 1 µl 10x Reaction buffer and 1 µl DNase (1U/µl) and incubated at 37°C for 30 min with shaking. 1 µl EDTA (50

mM) was added and incubated at 65°C for 10 min. After this step we added 1 µl of Random Hexamer Primers (0.2 µg/ µl) and the mixture was again incubated at 65°C for 5 min. Then a Master Mix containing following reagents was added to each sample:

Master Mix:

5x Reaction Buffer	4 µl
dNTPs (10mM)	2 µl
RiboLockTM RNase Inhibitor (Thermo, Germany)	1 µl
RevertAidTM Reverse Transcriptase (Thermo, Germany)	1 µl

Incubation protocol:

1st step:	25°C for 10 min
2nd step:	42°C for 1h
3rd step:	70°C for 10 min

cDNA was stored at -20°C.

3.3. Reverse Transcription PCR (RT-PCR)

The PCR was performed with the Qiagen® TaqDNA Polymerase Kit. The Kit was used according to the manufacture's introduction. The Master Mix was prepared on ice (for each sample):

During the whole preparation time the PCR tubes were stored on ice.

cDNA template (about 50 ng/µl)	2 µl
Sense primer (2 µM)	1 µl
Antisense primer (2 µM)	1 µl
dNTPs Mix (1mM)	2 µl
PCR Buffer, 10x	2 µl
Q-solution	4 µl
$MgCl_2$ (25mM)	1.25 µl
Taq Polymerase (5U/µl)	0.1 µl
Bidistilled H_2O	6.65 µl

For the amplification a Biometra TProfessional Thermocycler (Göttingen, Germany) was used with the following protocol:

1st step:	Denaturation	94°C for 5 min
2nd step:	Denaturation	94°C for 1 min
3rd step:	Annealing	60°C (*mErbb4*), 58°C (*Gapdh*) for 1min
4th step:	Extension	72°C for 1 min
5th step:	Extension	72°C for 1 min
5th step:	Cooling	4°C

Steps 2 to 4 were repeated 35 times before progressing to step 5 and 6 (36 cycles). PCR products were separated in a 1.5 % agarose TAE gel with ethidium bromide and visualized under UV light.

Primer:

mErbb4 sense:	5'-AAATGAAAGCTGGCGACGGG-3'
mErbb4 antisense:	3'-CAGAGTCATGTTGGAAGGCC-5'
Gapdh sense:	5'-GGTCGGAGTCAACGGATTTG-3'
Gapdh antisense:	3'-GTACTGGTGAAGCCGTAGCA-5'

3.4. Microarray analysis

For microarray analysis mice were bled under ether anesthesia and killed by cervical dislocation. Immediately the whole pancreas was infused with RNAlater (Sigma, Germany) and stored overnight in 5 ml RNAlater. Microarray analysis (G4858A SurePrint G3 Unrestricted GE 8x60K) (Agilent Technologies, Germany) was done in cooperation with the Laboratory of Functional Genome Analysis at the Gene Center in Munich.

3.5. Quantitative Real-time RT-PCR

Pancreas samples were homogenized in TRIzol® (Invitrogen, Germany) as described above for RNA isolation. 1 µg of RNA per sample was reverse transcribed in a final volume of 40 µl using RevertAid Reverse Transcriptase (Thermo, Germany) according to the manufacturer's instructions. Quantitative mRNA expression analysis was performed by real-time quantitative reverse-transcription polymerase chain reaction (RT-qPCR) using the LightCycler®480 System and the LightCycler®480 Probes Master (Roche, Germany). The primers had a concentration of 0.5 µM. The probe concentration was 0.2 µM. The final reaction volume was 10 µl, and cycle conditions were 95°C for 5 min for the first cycle, followed by 45 cycles of 95°C for 10 s, 60°C for 15 s, and 72°C for 1 s. The quantitative analysis is based on the detection of a signal associated with PCR products and the threshold cycle number at which the exponential increase of these PCR products could be detected for the first time. Based on these results the target gene results were related to the *Actb* content. Results are listed as fold differences in target gene expression relative to *Actb* transcripts. The ΔCt value of the sample was determined by subtracting the average Ct value of the target gene from the average Ct value of the *Actb* gene. Probes were labeled with the reporter dye FAM at the 5' and the quencher dye TAMRA at the 3' end. For each primer pair no-template control and no-RT control assays were performed, which produced negligible signals that were usually greater than 40 in Ct value. Experiments were performed in duplicates for each sample. Sequences of primers (Thermo Fisher Scientific, Germany) are shown in **Table 1**.

Table 1: Sequences of primers used for real-time quantitative PCR and probe numbers.

actin, beta	Forward Reverse Probe	5'-CGTGAAAAGATGACCCAGATCA-3' 5'-CACAGCCTGGATGGCTACGT-3' #5
albumin	Forward Reverse Probe	5'-ATCTGTCTGCAATCCTGAACC-3' 5'-ATGCTCACTCACTGGGGTCT-3' #84
serine (or cysteine) peptidase inhibitor, clade A, member 6	Forward Reverse Probe	5'-ACCTTAATCTCCCCAGTGAGC-3' 5'-CCTGGTGCTTAGGGACAGC-3' #81
matrix Gla protein	Forward Reverse Probe	5'-TGTTGCTTGCTCCTTACATGA-3' 5'-TACTTTCAACCCGCAGAAGG-3' #20
serine (or cysteine) peptidase inhibitor, clade F, member 1	Forward Reverse Probe	5'-GAGGCAGCTACTCCCCTCA-3' 5'-CTTCTCTCACAGCCTGCACTC-3' #1
matrix metallopeptidase 2	Forward Reverse Probe	5'-AGACACTGGTCGCAGTGATG-3' 5'-TGCCATCCTTCTCAAAGTTGT-3' #6
matrix metallopeptidase 3	Forward Reverse Probe	5'-AAGGGTCTTCCGGTCCTG-3' 5'-ATGCAATGGGTAGGATGAGC-3' #76
periostin, osteoblast specific factor	Forward Reverse Probe	5'-AAGCTCGGCAAGACAAG-3' 5'-TCAAATCTGCAGCTTCAAGG-3' #73
gastrin intrinsic factor	Forward Reverse Probe	5'-AGCTCATGGCCAGTGACAG-3' 5'-GGAGGACGTGAGAGCCATAA-3' #44

cadherin 11	Forward Reverse Probe	5'-TATACCACAGCCAGGCGTTT-3' 5'-CATGGAAAGAGGGATGCAG-3' #50
collagen, type I, alpha 1	Forward Reverse Probe	5'-AGCCCTGGTTCTCGAGGT-3' 5'-TCTTCGGGTAGCTCTGCTTG-3' #11
AE binding protein 1	Forward Reverse Probe	5'-TTCCCCTACACCAGCCATTA-3' 5'-CCTGCAGTGGTAGTGGGTAGA-3' #81
connective tissue growth factor	Forward Reverse Probe	5'-CACACCGCACAGAACCAC-3' 5'-TTCATGATCTCGCCATCG-3' #53
lumican	Forward Reverse Probe	5'-CAGCAACATTCCGGATGAG-3' 5'-TCATTGTGAGATAAACGCAGGT-3' #26
fibronectin 1	Forward Reverse Probe	5'-GACCCGGACATTTTACCAGA-3' 5'-TATCGGACACCATGCACAAA-3' #14
preproenkephalin	Forward Reverse Probe	5'-TACTGGGAACGGGAGACAAC-3' 5'-TTCGTCATTGTTGGTTGGTGCTCT-3' #83

4. Analysis of transgenic and knockout mice

Mice not used in pancreatitis experiments were also anesthetized with ether and blood was collected from the retroorbital sinus, in case the blood was needed for subsequent analysis of serum parameters. After that mice were killed by cervical dislocation. The abdominal cavity was opened carefully and the organs of interest were removed and stored under appropriate conditions for later studies.

4.1. Organ weight analysis

The removed organs were washed in 1x PBS, blotted dry on a paper towel and weighed to the nearest mg.

4.2. Body weight analysis

One day after birth pups were marked by foot tattooing and weighed for the first time. All animals were weighed weekly until the age of 8 or 12 weeks. Only littermates, separated by gender were compared.

4.3. Histological analysis

Organs were fixed for 24 hours in 4% paraformaldehyde (Sigma-Aldrich, Germany) solution at 4°C. Fixed tissues were dehydrated through a rising alcohol row and embedded in paraffin.

4% paraformaldehyde solution:

PBS	
Paraformaldehyd	4 %
5 M NaOH	0.025%

The solution was heated up to 50°C until the paraformaldehyde powder is completely in solution, and then the pH was adjusted to 7,4 by using HCl (Merck, Germany).

Before staining the sections the embedded tissue was cut with a microtome (Thermo, Germany) at a nominal thickness of 3 µm.

4.3.1. Hematoxylin/ eosin (H&E) staining

Sections were deparaffinized for 20 min in Roti®-Histol (Roth, Germany). Slides were rehydrated through a descending alcohol row (5 min, twice in 100 % ethanol, 2 min in 90 % ethanol, 2 min in 70 % and 2 min in 50% ethanol) and after that the slides were put for a short time in distilled water. The sections were stained for five minutes in Mayers Hemalaun (ready-to-use-solution). After that the sections were rinsed ten minutes in tap water to stain the nuclei. The slides were dipped five minutes into eosin (Sigma, USA), 10 times into 96% EtOH and 100% isopropanol to be dropped again in Roti®-Histol and finally mounted with Pertex (Labonord, Germany).

4.3.2. Immunohistochemical staining

Two hours before section mice were injected with BrdU (Roche, Germany) (30 mg/kg body weight) for cell proliferation analysis. The tissues were fixed, embedded, and mounted on superfrost glass microscope slides (Menzel Gläser, Germany), deparaffinized and rehydrated as described previously. After that the sections were treated with 3% H_2O_2 (Roth, Germany) for 15 minutes and washed shortly in distilled water. For antigen retrieval, the sections were boiled for 20 minutes in a 700 Watt microwave in a 10 mM sodium citrate buffer (pH 6.0).

Stock citrate acid (0.1 mol): 19.2 g citrate acid in 1 l bidistilled water

Stock sodium citrate (0.1 mol): 29.4 sodium citrate dihydrate in 1 l bidistilled water

Working solution:

citric acid (0.1 mol)	27 ml
sodium citrate (0.1 mol)	123 ml
Tween® 20	1.5 ml
bidistilled water up to	1500 ml

If the secondary antibody is biotin-conjugated the next step was to incubate them first for 15 minutes with an avidin solution (AXXORA GmbH, Germany) wash them shortly in TBS and incubate them again for 15 min in a biotin solution (AXXORA GmbH, Germany). The biotin solution was only dripped off. After that the tissue was covered with the primary antibody solution and incubated overnight at 4°C.

Following primary antibodies were used:
rabbit anti- ERBB4 (1:250 dilution, Santa Cruz, Germany)
rabbit anti-cleaved caspase-3 (1:200 dilution, Cell Signalling, Germany)
rat anti-Ki67 (1:200 dilution, Dako, Germany)
rat anti-BrdU (1:50 dilution, Serotec, Germany)

After the incubation of the primary antibody all slides were washed twice for 5 min in TBS and covered with the secondary antibody and incubated for 1 hour at room temperature (RT):
goat anti rabbit (1:100 dilution, Vektor BA 1000, USA)
rabbit anti rat (1:200 dilution, Dako E0468, Germany)

All slides were washed twice in TBS and covered with an avidin-biotin complex solution (AXXORA GmbH, Germany) diluted 1/100 for 30 min.
The slides were washed again in TBS and were finally covered with 3,3‘-diaminobenzidine (DAB) (KEN-EN-TEC, Denmark) as a chromogen, as long as the staining is strong enough. 1% H_2O_2 (Roth, Germany) was added per ml DAB to start the reaction. The staining reaction was stopped by washing the slides in bidistilled water. Next, the sections were stained in hematoxylin solution (Mayer, Germany) for 30 seconds, rinsed under running tap water for 5 min, dehydrated to Roti®-Histol and mounted with Pertex (Labonord, Germany) and cover slides.

<u>10x TBS:</u>

NaCl	80g
Tris	30g
Bidistilled water up to	1l
Adjusted to pH 7.4	

4.3.3. X-Gal staining

Ptf1a-Cre mice were crossbred with *Gt (ROSA)26Sor*$^{tm/Sor}$ mice, which carry a modified *LacZ* gene driven by the cell type-independent *ROSA26* promoter. The Cre enzyme excises a stop cassette upstream of *LacZ* and thereby activates the expression of ß-galactosidase. The ß-galactosidase marks cells in which *Ptf1a* is expressed and the active ß-galactosidase-expressing locus is inherited by their progeny. To detect these cells the histological sections have to be stained with 5-bromo-4-chloro-3-indolyl-ß-$_D$-galactoside (X-Gal) (Invitrogen, Germany) (Kawaguchi, 2002 #68). This enzyme cleaves the disaccharide lactose, releasing galactose und glucose. However it is also able to cleave the synthetic substrate X-Gal, resulting in an indigo color.

Pancreas and kidney of wildtype and *Ptf1a-Cre/Gt (ROSA)26Sor*$^{tm/Sor}$-mice were incubated for 10 min in the fixative at 4°C and then embedded in Tissue OCT. 8 µm sections were obtained with a cryostat.

Fixative:

6.7 ml	3 % glutaraldehyde
2.7 ml	37% formaldehyde
20 µl	NP40
90.5 ml	PBS

Staining protocol:

Sections were air-dried and fixed for 30 min in ice-cold acetone at RT.
After that the sections were washed in 1 x PBS and stained overnight at 37°C in the following staining solution.

Staining solution:

46.9 ml	PBS
100 µl	$MgCl_2$ (1M)
50 mg	sodiumdeoxycholate
10 µl	NP40
500 µl	$K_3Fe(CN)_6$ (500mM)
500 µl	$K_4Fe(CN)_6$ x 3 H_2O (500mM)
2 ml	X-Gal (50mg/ml)

The next day all slides were washed twice in PBS, stained shortly in eosin, dehydrated to Roti®-Histol and mounted with Pertex and cover slides.

4.3.4. Proliferation and apoptosis indices

For the identification of proliferating and apoptotic cells in the pancreas we used BrdU or Ki67 (proliferation) and cleaved caspase-3 (apoptosis) immunohistochemical staining of the pancreas. The numerical area density of proliferating or apoptotic cells were calculated by dividing the total number of immunostained cell nuclei of the exocrine pancreas by the whole number of cell nuclei of the exocrine pancreas. Therefore we measured the cross-sectional area of the whole pancreas and counted the cell nuclei of one visual field. For these measurements a Videoplan Image Processing System (Leica Application Suite Software, Germany) coupled to a microscope (Leica, Germany) via a color video camera (Leica DFC425, Germany) was used. The measurement was carried out with a 25x objective providing an 850x final magnification. The area of the exocrine pancreas was measured by tracing its contour with the courser. The image analysis system is the able to determine the exact area of the chosen surface.

5. Protein analysis

5.1. Sample collection

Mice were killed by cervical dislocation and tissue samples for protein analysis were snapfrozen and stored at - 80°C until needed.

5.2. Extraction of protein from tissue

Samples stored at -80°C were first weighed and homogenized for 1 minute with a tissue homogenizer (Miccra, ART Labortechnik, Germany). The tissues were homogenized in protein extraction buffer (for 20 mg of tissue 500 µl extraction buffer was used) by 23500 rpm. After each sample the homogenizer was cleaned with distilled water and PBS.

5x Laemmli buffer:	1 M Tris (pH 6.8)	65.5 ml
	Glycerol	100 ml
	0.5M EDTA (pH 8.0)	2 ml
	SDS	20 g
	Bromophenol blue	0.1%
	Bidistilled water up to	200 ml
Protein extraction buffer:	1M Tris (pH 7.5)	2 ml
	Tween®	2 ml
	5x Laemmli buffer	20 ml
	Bidistilled water	76 ml

5.3. Pancreatic cell fractionation

The fractionation was performed with the QIAGEN Qproteome® Cell Compartment Kit according to the manufacturer's instructions. The used buffers (CE1, CE2, and CE3) were treated with 1% protease inhibitor. 49 µl of benzonase to 91 µl bidistilled water were added. All solutions were cooled on ice and all steps of the fractionation were performed at 4°C.

Pancreas samples stored at -80°C were put on dry ice until starting the cell fractionation. First the tissue was washed in 1 ml ice-cold PBS and split into pieces of 20 to 26 mg. These pieces were homogenized for 5 s in a tissue homogenizer in 500 µl CE1 buffer. The suspension was transferred into Qiagen shredder homogenizer tubes and centrifuged at the lowest power for 2 min. The pellet was carefully resuspended in the supernatant of the collection tube using a pipette. The content was transferred into a new centrifuge tube and filled with 500 µl ice-cold CE1 buffer. In the next step the centrifuge tubes were rotated in an overhead shaker for 10 min and subsequently centrifuged at 4000x g for another 10 min. The supernatant (fraction 1) containing cytoplasmic proteins was pipetted into a fresh centrifuge tube and stored on ice. 1 ml CE2 buffer was used for resuspending the pellet. The resuspended sample was rotated using an overhead shaker for 30 sec, after that centrifuged at 6000x g for 10 min to receive the fraction 2 in the supernatant. The fraction 2 consists of membrane proteins. The pellet was again resuspended with 20 µl of benzonase solution by snapping against the centrifuge tube and left at room temperature for 15 min. Finally, 500 µl of CE3 buffer were added, the pellet was resuspended by pipetting and the sample was mixed in an overhead shaker for 10 min at 4°C. To finish this step it was centrifuged by 6800 x g for 10 min at 4°C. The supernatant contains the nuclear proteins (fraction 3). For later protein concentration determination the samples have to be dissolved in protein extraction buffer. Therefore the samples were mixed with a 4-fold proportion of ice-cold acetone and incubated at RT for 15 min. The samples were centrifuged at 12000x g for 10 min at 4°C. After the supernatant was carefully discarded, the pellet was dried in a vacuum centrifuge for 10 min. Fraction 1 and 2 were resuspended in 180 µl, fraction 3 in 120 µl protein extraction buffer.

5.4. Determination of the protein concentration

To determine the protein concentration of the samples a bicinchoninic acid (BCA) assay was performed. We used a stock solution (4 mg/ml) of bovine serum albumin (Roth, Germany) and serial dilutions to create a standard curve. 50 µl of the standard and the samples of unknown concentration (1:10 dilution in PBS) were pipetted in a 96-well plate. 200 µl of a mixture of BCA and 4 % $CuSO_4$ (Sigma-Aldrich, Germany) were added to each well. After that the plate was incubated at 37°C for 30 min to measure the absorbance at 562 nm. The standard curve was created by plotting the absorbance of the standards versus their known protein concentrations and used to calculate the unknown concentrations of the protein samples.

5.5. SDS-Polyacrylamide gel electrophoresis (SDS-PAGE)

20 µg of protein of each sample were pipetted into centrifuge tubes and filled up with 1xLaemmli buffer to attain the same volume. In some experiments it was necessary to add 5% of 2-mercaptoethanol (Merck, Germany) to the samples. All samples were incubated at 95°C for 5 min and after that stored on ice. Protein separation was performed using the Mini Protean® 3 cell system (Bio Rad, Germany). To prepare the separating gel a 50 ml glass beaker was used. Under continuous agitation the different substances were added and poured into the space between the glass plates of the system, leaving enough space for the stacking gel (about 2.5 cm). The polymerization process lasts 1 hour. To ensure an even surface the separating gel it was covered with bidistilled water. After complete polymerization the water was discarded and the stacking gel was prepared and poured on top of the separating gel and a comb was inserted. After complete polymerization of the stacking gel (30 min), the plates were connected to the electrophoresis chambers, filled with SDS-PAGE electrophoresis buffer and the comb was removed. A molecular weight standard (MBI Fermentas, PageRuler™ Prestained Protein Ladder #SM0671, Germany) was pipetted into the first well. Samples were then loaded and the electrophoresis was performed initially at 100V for 10 min and then at 140V until the bromophenol blue front left the separating gel.

separating gel:	bidistilled water	3.35 ml
	1.5 M Tris	2.5 ml
	30% acrylamide	4.0 ml
	10% SDS	100 µl
	10% ammoniumpersulfate	50 µl
	Temed	5 µl

stacking gel:	bidistilled water	7.0 ml
	1.5 M Tris	1.25 ml
	30% acrylamide	1.5 ml
	10% SDS	100 µl
	10% ammoniumpersulfate	100 µl
	Temed	5 µl

SDS-PAGE electrophoresis buffer:	Tris	30.3 g
	Glycine	144 g
	SDS	10 g
	bidistilled water up to	1 l

5.6. Electrophoretic blotting

A semidry electro blotting apparatus (Bio-Rad, Germany) was used to transfer the separated proteins to a PVDF membrane (Millipore). The gel blotting paper (Bio-Rad, Germany) in the same size of the gel was soaked in 1x transfer buffer and placed on the bottom of the electrode. The blotting paper was covered with the membrane and the gel exactly in the same position. On top we placed again a sheet of blotting paper soaked with transfer buffer. To eliminate air bubbles we used an empty test tube to squeeze carefully the whole construct. The upper electrode was put on the blotting apparatus and connected to a power supply (Bio-Rad). The blotting procedure took place 1 hour at 15 mA. After the transfer the membranes were immediately lettered with a pen, not solvable in methanol and stained in Ponceau S (Sigma, Germany). The membranes were carefully dried and stored at 4°C.

10x transfer buffer:	Tris	58.2 g
	Glycine	29.2 g
	SDS	3.7 g
	bidistilled water up to	1 l

5.7. Detection of the antigen

To activate the membranes with the transferred proteins, they were rinsed 1 min in methanol and then washed 3 times for 5 min in TBS-T buffer at RT in a hybridization oven (Bachofer, Germany). The next step was to incubate the membranes in blocking solution for one hour again at RT in a hybridization oven without heating. The blocking solution, either instant skimmed milk (Roth, Germany) or BSA (Roth, Germany), was matched to the solution in which the secondary antibody was diluted. After that the primary antibody was diluted in 2.5% milk or 5% BSA in TBS-T. If the primary antibody was not diluted in the same solution as in the step before, the membranes were washed 4 times for 5 min in TBS-T. The incubation of the primary antibody took place overnight and at 4°C. At the next day all membranes were rinsed 3 times in TBS-T before the 1 hour lasting incubation with the secondary antibody could be started. Before the detection process the membranes were washed 3 times for 5 min in TBS-T. Detection was performed by incubating the membranes 1 min with 2 ml of ECL detection reagent (GE Healthcare, Germany) the membrane was covered with plastic and exposed to an ECL film (GE Healthcare, Germany).

10x TBS buffer:	Tris	30 g
	NaCl	80 g
	Bidistilled water up to	1 l

TBS-T buffer:	1x TBS
	0.1 % Tween 20

blocking solution:	2.5 or 5% instant skimmed milk powder or BSA in TBS-T

Primary antibodies:

Goat anti-SerpinA6 (1:1000 dilution in 2.5% BSA, AF: 4065 (R&D, Germany))
Rabbit anti-SerpinF1 (1:1000 dilution in 2.5% BSA, QC0455 (Sigma-Aldrich, Germany))
Rabbit anti-44/42 MAPK (1:2000 dilution in 5% BSA, 9102 (Cell Signalling, Germany))
Rabbit anti-phospho 44/42 MAPK (1:2000 dilution in 5% BSA, 4370 (Cell Signalling, Germany))
Rabbit anti-Akt (1:1000 dilution in 5% BSA, 4691 (Cell Signalling, Germany))
Rabbit anti-phospho-Akt (1:2000 dilution in 5% BSA, 4060 (Cell Signalling, Germany))
Rabbit anti-Erbb2 (1:1000 dilution in 2.5% milk powder, 284 (Santa Cruz, Germany))
Rabbit anti-HistoneH3 (1:1000 dilution in 5% BSA, 9717 (Cell Signalling, Germany))
Mouse anti-Erbb4(C-7) (1:1000 dilution in 2.5% milk powder, 8050 (Santa Cruz, Germany))
Rabbit anti-GAPDH (1:5000 dilution in 5% BSA, 2118 (Cell Signalling, Germany))

Secondary antibodies:

Donkey anti-goat (1:1000 dilution in 5%BSA, HAF: 109 (R&D, Germany))
Donkey anti-rabbit (1:2500 dilution in 5% milk powder, NA: 934V (GE Healthcare, Germany))
Rabbit anti-mouse (1:2500 dilution in 5% milk powder, 7076 (Cell Signalling, Germany))

6. Acute pancreatitis

6.1. Caerulein-induced pancreatitis model

All mice were placed for 18 h on a special grid for fasting, water was offered *ad libitum*. Two different protocols were used. A 3 hour lasting pancreatitis was induced by two intraperitoneal (i.p.) injections of caerulein (Sigma, USA) (50 µg caerulein/kg mouse, dissolved in 0.9% NaCl) and the animals were killed 3 hours after the first injection. A 24 hour lasting pancreatitis was induced by 8 injections of caerulein and the mice were killed 24 hours after the first injection. After the last caerulein injection the fasting-grid was removed and food was offered *ad libitum*. Before the mice were killed by cervical dislocation they were anesthetized in ether and blood was collected for serum analysis from the retroorbital sinus. The mice were dissected carefully and the whole pancreas was extracted. First three small samples of different parts of the pancreas were collected and immediately frozen on dry ice for protein analysis. Again three samples, but smaller than those for protein analysis, were taken out of three different parts of the pancreas and homogenized in RLT buffer (Qiagen, Germany) with 1% 2-mercaptoethanol and frozen in liquid nitrogen. For histological analysis the remaining part of the pancreas was fixed for 24 h in 4 % PFA at 4°C and embedded in paraffin.

6.2. L-arginine pancreatitis model

To make sure that the results of the caerulein-induced pancreatitis are reproducible in other pancreatitis models we also performed the L-arginine pancreatitis model. For the L-arginine model of pancreatitis non-fasted mice were used. Pancreatitis was induced by i.p. application of 4 g/kg arginine per body weight (Sigma, Germany). A sterile solution of L-arginine hydrochloride (8%) was prepared in 0.9% NaCl (B.Braun, Germany). The pH of this solution was adjusted to 7.0. Mice received 2 injections of L-arginine (4 g/kg). Blood was collected under ether anaesthesia at 0, 24, 48, and 72 hours after the first injection from the retroorbital sinus. After that the mice were sacrificed and tissue samples were removed and further processed.

6.3. Pain treatment with metamizole

Because pancreatitis is a very painful disease we treated all mice used in pancreatitis experiments with 70 mg/kg metamizole (Vetalgin®) (Intervet, Germany). Metamizole does not influence the caerulein-induced inflammation (Stumpf, unpublished). The metamizole applications were given orally before the first caerulein injection and 4, 8, 12 and 20 hours after starting the experiment (Fig.3.1).

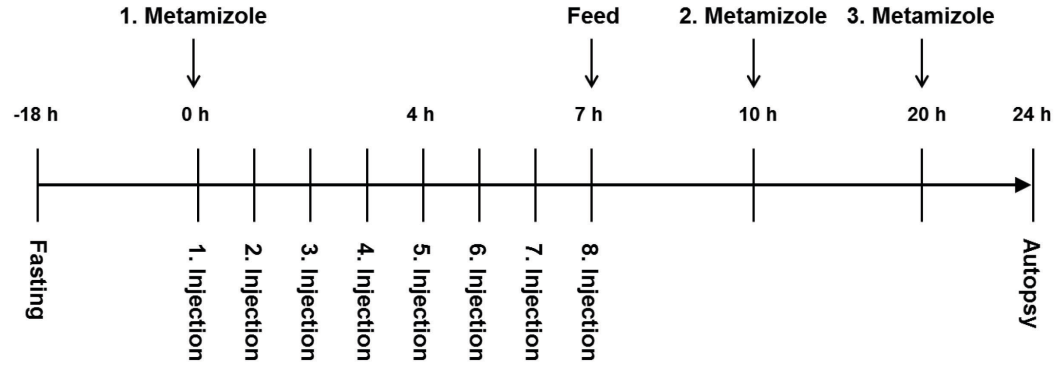

Figure 3.1: Metamizole treatment of mice used in pancreatitis experiments.

6.4. Serum analysis

Blood collected from the retroorbital sinus was allowed to clot for 1h at 4°C and then centrifuged for 10 min at 1700x g. The serum was separated from the remaining components of the blood and was pipetted in a separate centrifuge tube and was stored at -80°C. For measuring the serum parameters amylase and lipase the serum samples were diluted 1:10 with 0.9% NaCl (B.Braun, Germany) and stored on dry ice until needed for the measurement. The measurement was performed by the institute “Klinische Chemie” of the “Klinikum Rechts der Isar”, Munich.

6.5. Histological scoring

To evaluate the three major parameters of AP (necrosis, inflammation and edema), a special histological score was generated. To perform this score H&E-stained histological pancreatic sections of 3 µm were prepared. The pancreas was

cut in longitudinal sections five times in a distance of 25 µm. The sections were stained in H&E and graded in a blinded manner. To evaluate the severity of the edema, the necrosis and the inflammatory cell infiltration in 20 visual fields of each surface of the slides were examined and estimated. The 50x magnification was used for the edema and the 400x (HPF) for the inflammation and the necrosis. The histological score was performed as described below:

Edema:

0 = absent
0.5 = focal expansion of interlobar septae
1 = diffuse expansion of interlobar septae
1.5 = same as 1 + focal expansion of interlobular septae
2 = same as 1 + diffuse expansion of interlobular septae
2.5 = same as 2 + focal expansion of interacinar septae
3 = same as 2 + diffuse expansion of interacinar septae
3.5 = same as 3 + focal expansion of intercellular septae
4 = same as 3 + diffuse expansion of intercellular septae

Acinar necrosis:

0 = absent
0.5 = focal occurrence of 1-4 necrotic cells/HPF
1 = diffuse occurrence of 1-4 necrotic cells/HPF
1.5 = same as 1 + focal occurrence of 5-10 necrotic cells/HPF
2 = diffuse occurrence of 5-10 necrotic cells/HPF
2.5 = same as 2 + focal occurrence of 11-16 necrotic cells/HPF
3 = diffuse occurrence of 11-16 necrotic cells/HPF
3.5 = same as 3 + focal occurrence of >16 necrotic cells/HPF
4 = diffuse occurrence of >16 necrotic cells/HPF

Inflammation:

0 = 0-1 intralobular leukocytes/HPF

0.5 = 2-5 intralobular leukocytes/HPF

1 = 6-10 intralobular leukocytes/HPF

1.5 = 11-15 intralobular leukocytes/HPF

2 = 16-20 intralobular leukocytes/HPF

2.5 = 21-25 intralobular leukocytes/HPF

3 = 26-30 intralobular leukocytes/HPF

3.5 = 30-35 intralobular leukocytes/HPF

4 = >35 intralobular leukocytes/HPF

7. Statistical analysis

The statistical analysis was performed with a two-tailed student's *t*-test except for the results of the qRT-PCR study. The qRT-PCR data were analyzed with a two-tailed Mann-Whitney *U*-test. All Data are presented as means ± SD or mean ± SEM (histological scoring) and graphs were generated with Prism 4.0. Quantitative RT-PCR values were related to the mean value of the control group and data are presented as box plots with medians. All results were analyzed for significance (Graph Pad Prism 4.0 for Windows, Graph Pad Software, and USA). Differences were considered statistically significant if $P < 0.05$.

8. Material

8.1. Equipment

Accu-jet® pro pipette controller	Brand, Wertheim, Germany
Agarose gel electrophoresis chamber	MWG-Biotech, Ebersberg, Germany
Agarose gel electrophoresis power	Bio Rad, Munich, Germany
Blunt forceps	Aesculap, Tuttlingen, Germany
Bulldog forceps	Aesculap, Tuttlingen, Germany
Centrifuges 5417, 5417R	Eppendorf, Hamburg, Germany
Chyo JL-200 (analytical balance)	Chyo, Japan
Chyo MJ-3000 (analytical balance)	Chyo, Japan
Color video camera (DFC425)	Leica, Wetzlar, Germany
Curix60 Tabletop processor	Agfa HealthCare, Greenville, USA
Duran®-Schott glass ware	DURAN Group, Wertheim, Germany
Electrophoresis chamber	MWG-Biotech, Ebersberg, Germany
ELISA reader Spectra Max 250	Molecular Devices, Sunyvale, USA
EPS 500/400 Electrophoresis Power Supply	Pharmacia Fine Chemicals, NJ, USA
Fine scissors	Aesculap, Tuttlingen, Germany
Gel documentation system	Intas, Göttingen, Germany
GeneAmp PCR System 9700	Applied Bisosystems, Foster City, USA
Glass case for glass rack	Roth, Karlsruhe, Germany
Glucometer	Abott, Ludwigshafen, Germany
Heating plate with magnetic stirrer	IKA process equipment, Staufen, Germany
Homogenizer Miccra	ART Labortechnik, Müllheim, Germany
Hybridization oven	Bachofer, Reutlingen, Germany
Laboratory scale, BP221S	Sartorius, Göttingen, Germany
Laboratory scale, BP4100S	Sartorius, Göttingen, Germany

Laminar flow cabinet	BDK, Sonnenbühl-Genkingen, Germany
LightCycler 480	Roche, Mannheim, Germany
MicroPlate reader	Tecan, Männedorf, Swizzerland
Microtome	Microm, Walldorf, Germany
Microscope	Leica, Wetzlar, Germany
Microwave	Siemens, Munich, Germany
Mini Protean® 3 Cell	Bio Rad, Munich, Germany
MS1 Minishaker	IKA process equipment, Staufen, Germany
NanoDrop-1000 spectrophotometer	NanoDrop Technologies, Wilmington USA
PCR-machine/thermal cycler	Biometra, Göttingen, Germany
PIPETMAN® P (1000µl)	Gilson, Limburg, Germany
PIPETMAN® P (100µl)	Gilson, Limburg, Germany
PIPETMAN® P (10µl)	Gilson, Limburg, Germany
PIPETMAN® P (200µl)	Gilson, Limburg, Germany
PIPETMAN® P (20µl)	Gilson, Limburg, Germany
PIPETMAN® P (2µl)	Gilson, Limburg, Germany
Pointed scissors	Aesculap, Tuttlingen, Germany
Power Pac 300	Bio Rad, Munich, Germany
Power Supply PPS200-1D	MWG-Biotech, Ebersberg, Germany
Rotating shaker	Infors AG, Bottmingen, Germany
Semidry electroblotting apparatus	Bio-Rad, Munich, Germany
Spectrophotometer	Beckman, Palo Alto, USA
Table centrifuge (5417R)	Eppendorf, Hamburg, Germany
Thermomixer 5436	Eppendorf, Hamburg, Germany
Thermocycler TProfessional	Biometra, Göttingen, Germany
Ultraschall Sonorex Super RK 102 H	Bandelin, Berlin, Germany
UV-Crosslinker	Biometra, Göttingen, Germany
VakuLab s3000 (Autoclave)	MMM group, München, Germany
Watch maker forceps	Aesculap, Tuttlingen, Germany
Water bath SUB14	Grant Instruments, Royston, Great Britain

8.2. Consumables

96-well cell culture plates (flat-based)	BD, Heidelberg, Germany
96-well real-time PCR plates	Eppendorf, Hamburg, Germany
Blotting paper	Bio-Rad, Munich, Germany
Centrifugation tube (15 ml, 50 ml)	Becton Dickinson, Heidelberg, Germany
Centrifuge tube (0.5 ml, 1.5 ml, 2.0 ml)	Eppendorf, Hamburg, Germany
Chemoilluminiscence film	GE Healthcare, Munich, Germany
Cover glass slides	VWR International, Darmstadt, Germany
Cryotube 1.0 ml	Nunc A/S, Roskilde, Denmark
Filter paper	GE Healthcare, Munich, Germany
Glass microscope slides	Menzel-Gläser, Braunschweig, Germany
Heat sealing foil	Eppendorf, Hamburg, Germany
Heparinized capillary tubes	Brand, Gießen, Germany
Histology cassettes	Medite, Burgdorf, Germany
Microarrays	Agilent Technologies, Germany
PCR-reaction-tubes	G. Kisker GbR, Steinfurt, Germany
Petri dishes (diameter 10 cm)	Becton Dickinson, Heidelberg, Germany
Plastic tubes (5 ml)	Greiner Bio-One, Frickenhausen, Germany
PVDF membrane	Millipore, Billerica, USA
Real-time PCR plates (96 well)	Eppendorf, Hamburg, Germany
Rundbodenröhrchen, 5 ml	Falcon/BD, Heidelberg, Germany
Standard rodent chow	Ssniff, Soest, Germany
Sterican® cannulas (18G, 20G)	B.Braun, Melsungen, Germany
Superfrost slides	Menzel, Braunschweig, Germany
Syringes (2, 5, 10, 20 ml)	Codan Medical ApS, Roedby, Denmark
Uni-Link embedding cassettes	Engelbrecht, Edermüde, Germany

8.3. Chemicals

0.9% NaCl solution	B.Braun, Melsungen, Germany
2-mercaptoethanol	Merck, Darmstadt, Germany
ABC (Avidin-biotin complexes)	Vector Laboratories, Burlingame, USA
Acetone	CLN, Niederhummel, Germany
Acrylamide, 30%	Bio-Rad, Munich, Germany
Agarose	Invitrogen, Karlsruhe, Germany
Amersham ECL WB Detection Reagent	GE Healthcare, Munich, Germany
Ammonium persulfate, 10%	Bio-Rad, Munich, Germany
Bichinonic acid	Sigma-Aldrich, Deisenhofen, Germany
BrdU	Roche, Mannheim, Germany
Bromphenol blue	Serva, Heidelberg, Germany
BSA	Roth, Karlsruhe, Germany
Caerulein	Sigma, St. Louis, USA
Chloroform	Merck, Darmstadt, Germany
Collagenase II	Biochrom, Berlin, Germany
$CuSO_4$	Sigma-Aldrich, Deisenhofen, Germany
DEPC	Sigma-Aldrich, Deisenhofen, Germany
DNA Rehydration Solution	Promega, Mannheim, Germany
DNase I Amp Grade, 1U/µl	Invitrogen, Karlsruhe, Germany
DNase I reaction buffer, 10x	Invitrogen, Karlsruhe, Germany
DNase I, Amplification Grade	Invitrogen, Karlsruhe, Germany
dNTPs (dATP, dTTP, dCTP, dGTP)	MBI Fermentas, St. Leon-Rot, Germany
DTT, 0.1 M	Invitrogen, Karlsruhe, Germany
ECL solution (#34076; #34077)	Thermo Scientific, Rockford, USA
EDTA	VWR International, Darmstadt, Germany
EDTA solution, 25 mM	Invitrogen, Karlsruhe, Germany

Enzyme mix	Roche, Mannheim, Germany
Eosin Y	Sigma, St.Louis, USA
Ethanol	Merck, Darmstadt, Germany
Ethanol 99% with 2-Butanon 1%	HEMA GmbH, Nürnberg, Germany
Ethidiumbromide	Roth, Karlsruhe, Germany
Glacial acetic acid	Roth, Karlsruhe, Germany
Glycine	Merck, Darmstadt, Germany
Glycerine	Roth, Karlsruhe, Germany
Glucose solution	B.Braun, Melsungen, Germany
HCl	Merck, Darmstadt, Germany
H_2O_2	Roth, Karlsruhe, Germany
Hematoxylin solution according to Mayer	Sigma-Aldrich, Deisenhofen, Germany
Hot-start Taq, 5 U/µl	Quiagen, Hilden, Germany
Instant skimmed milk powder	Roth, Karlsruhe, Germany
Isopropanol p.a.	Merck, Darmstadt, Germany
Isopropanol, technisch	Roth, Karlsruhe, Germany
KCl	Roth, Karlsruhe, Germany
KH_2PO_4	Merck, Darmstadt, Germany
L-arginine hydrochloride	Sigma, Deisenhofen, Germany
Loading dye (6x)	MBI Fermentas, St. Leon-Rot, Germany
Methanol	Merck, Darmstadt, Germany
$MgCl_2$, 25 mM	Invitrogen, Karlsruhe, Germany
$MgCl_2$, 25 mM	Qiagen, Hilden, Germany
Molecular weight marker	MBI Fermentas, St. Leon-Rot, Germany
Na_2HPO_4	Merck, Darmstadt, Germany
NaCl	Roth, Karlsruhe, Germany
NaOH	Roth, Karlsruhe, Germany
Nuclei Lysis Solution	Promega, Mannheim, Germany
PageRulerTMPrestained Protein Ladder	MBI Fermentas, St. Leon-Rot, Germany
Paraformaldehyde	Sigma-Aldrich, Deisenhofen, Germany

Path Tissue Oct	LABONORD S.A.S, Gutenberg, Germany
PCR buffer with $MgCl_2$, 10x	Roche, Mannheim, Germany
PCR buffer, 10x	Qiagen, Hilden, Germany
Pertex (mounting medium)	Medite, Burgdorf, Germany
Ponceau S Solution	Sigma, Deisenhofen, Germany
Protein Precipitation Solution	Promega, Mannheim, Germany
Proteinase K	Roche, Mannheim, Germany
pUC mix molecular weight marker	MBI Fermentas, St. Leon-Rot, Germany
Q-Solution	Qiagen, Hilden, Germany
Rabbit serum	PromoCell, Heidelberg, Germany
Random hexamer primer	Invitrogen, Karlsruhe, Germany
RLT buffer	Qiagen, Hilden, Germany
RNAlater®	Sigma, Deisenhofen, Germany
Rnase	Roche, Mannheim, Germany
RNeasy Mini kit	Qiagen, Hilden, Germany
Roti®-Histol	Roth, Karlsruhe, Germany
RT buffer, 10x	Invitrogen, Karlsruhe, Germany
SDS	Serva, Heidelberg, Germany
Sigma Fast DAB Tablet Set	Sigma-Aldrich, Taufkirchen, Germany
Sodium citrate	Merck, Darmstadt, Germany
Skimmed milk powder	Roth, Karlsruhe, Germany
Taq DNA polymeras Kit	Quiagen, Hilden, Germany
Taq Polymerase, 5 U/µl	Quiagen, Hilden, Germany
Temed	Bio-Rad, Munich, Germany
Tris	Roth, Karlsruhe, Germany
TRizol® reagent	Invitrogen, Karlsruhe, Germany
Tween®20	Sigma-Aldrich, Deisenhofen, Germany
Vectastain Elite ABC Kit	AXXORA GmbH, Lörrach, Germany
Washing buffer	Roche, Mannheim, Germany
X-gal	Invitrogen, Karlsruhe, Germany

8.4. Drugs

0.9% NaCl solution	B.Braun, Melsungen, Germany
Diethyl ether	Carl Roth GmbH, Karlsruhe, Germany
Histoacryl® liquid skin glue	B.Braun, Melsungen, Germany
Metamizole-Sodium (Vetalgin®)	Intervet, Unterschleißheim, Germany

8.5. Software

Agilent Microarray	Agilent Technologies, Inc., Santa Clara, USA
GraphPad 4.0 software	GraphPad, LaJolla, USA
Microsoft Office 2007	Microsoft, Redmond, USA
Videoplan Image Processing System	Leica Application Suite Software, Weztlar, Germany

IV. RESULTS

1. Is the protective effect of BTC during AP mediated by the EGFR?

1.1. Generation of *Btc* transgenic mice in an *Egfr*-deficient background (*Btc*+*Wa5*)

To obtain *Egfr*$^{+/Wa5}$ (*Wa5)* mice with additional ubiquitous BTC-overexpression we crossbred *Wa5* mice with *pTORU-Btc* mice (L2). These double transgenic mice show a severe impairment in the function of the EGFR (dead kinase receptor) and ubiquitous BTC-overexpression.

1.2. Investigation of *Btc*+*Wa5* mice during caerulein-induced pancreatitis

To investigate if the protective effect of BTC in AP is EGFR-dependent, the caerulein pancreatitis model was used to evaluate the consequences of the loss of EGFR function in mice with ubiquitous BTC-overexpression. A 24-hour-lasting pancreatitis was induced by 8 injections of caerulein and the mice were killed 24 hours after the first injection. The 3-month-old male mice were fasted for 18 hours before starting the experiment. The serum markers of pancreatitis, serum amylase and lipase, were measured for all genotypes (*Btc, Wa5, Btc+Wa5* and WT) (Fig. 4.1). The chemical analysis of serum after the 24-h-lasting pancreatitis showed significantly reduced values of amylase and lipase in *Btc* transgenic mice and *Btc+Wa5* mice compared to wildtype and *Wa5* mice.

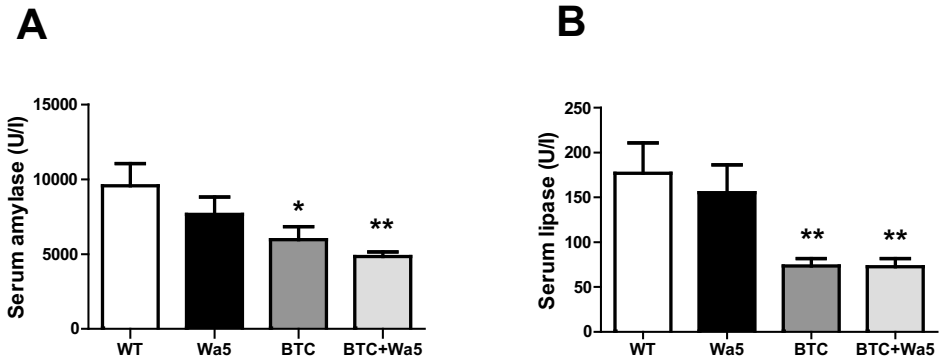

Figure 4.1: Serum amylase (A) and lipase (B) levels of the four animal groups (*Btc, Wa5, Btc+Wa5* and WT) after a 24-h-lasting pancreatitis (male, aged 3 months), (n=6/group), *: $P<0.05$, **: $P<0.01$.

A histological scoring was employed to evaluate the number of necrotic and inflammation cells and the grade of edema to estimate the grade of induced AP. 50 visual fields per animal and H&E-stained pancreas were evaluated. BTC-overexpressing mice as well as *Btc+Wa5* were protected, indicating that the protective effect of BTC is EGFR-independent (Fig. 4.2 and Fig. 4.3).

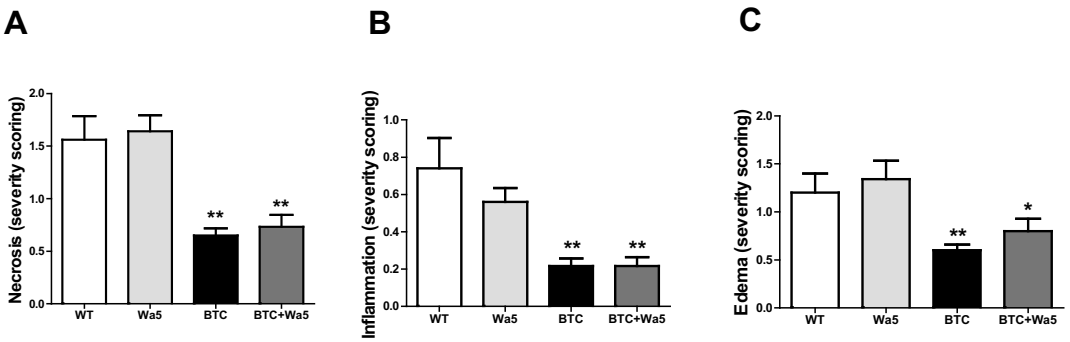

Figure 4.2: Histological scoring shows that the protective effect of BTC is not influenced by the loss of EGFR. Evaluation of the necrotic cells (A) the inflammation cells (B) and the edema (C) in the four animal groups (*Btc, Wa5, Btc+Wa5* and WT) after a 24-hour-lasting pancreatitis (n=6/group), *: $P<0.05$, **: $P<0.01$.

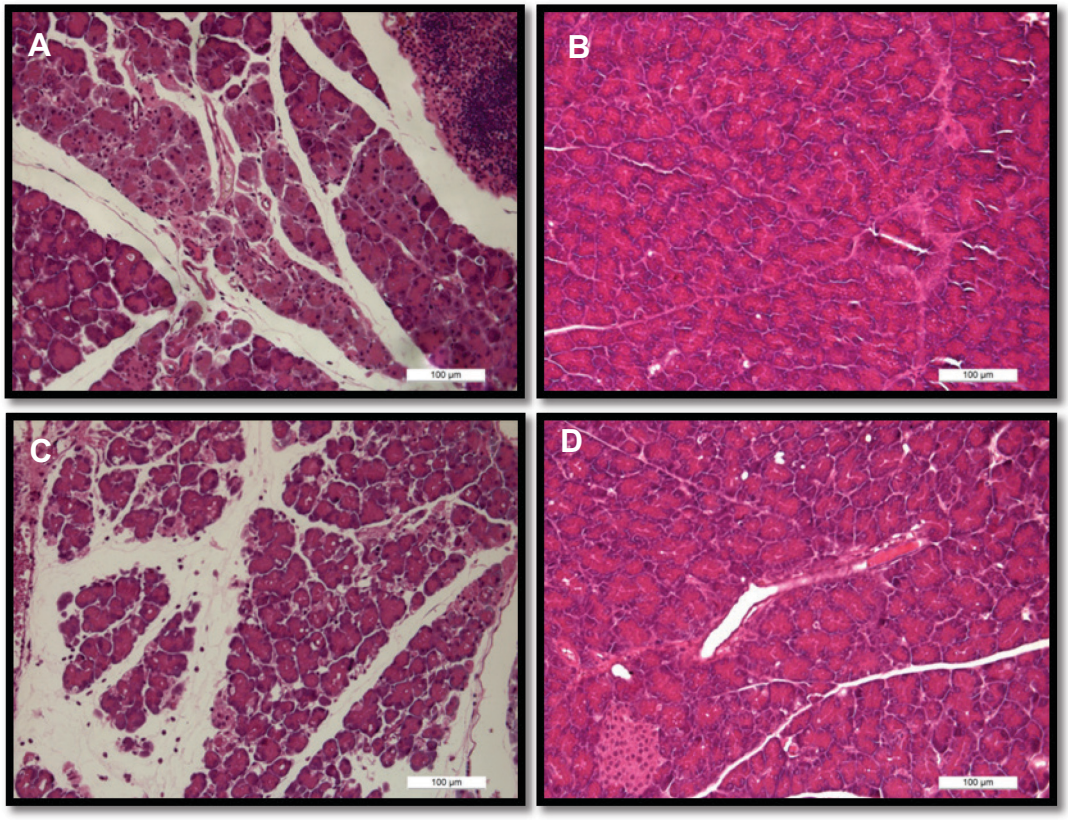

Figure 4.3: Examples of H&E-stained histological sections employed for the scoring of necrosis, inflammation and edema. Wildtype (A) and *Wa5* mice (C) show the main indications of AP with invasion of inflammation cells, necrosis and edema. *Btc* transgenic mice (B) and *Btc+Wa5* mice (D) are protected, (male, aged 3 months). Scale bar represents 100 µm.

1.3. Determination of the apoptosis rate after a 3-h-lasting caerulein-induced pancreatitis in *Btc+Wa5* mice

Previous studies revealed that apoptosis may be a main reason for the protective effect of BTC in AP. To determine the apoptosis rate we used 11-week-old male animals subjected to a 3-hour-lasting caerulein-induced pancreatitis. The 3-hour-lasting pancreatitis was induced by two injections of caerulein and the animals were killed 3 hours after the first injection. The number of positive cells was significantly increased in both *Btc* and *Btc+Wa5* mice (Fig. 4.4).

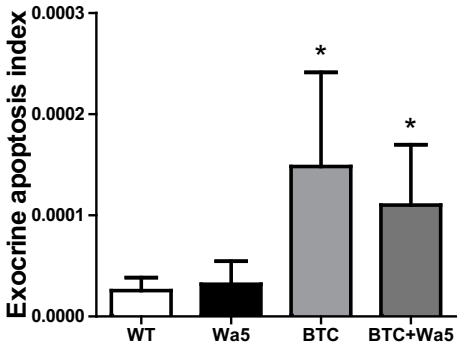

Figure 4.4: Cell apoptosis in the exocrine pancreas after pancreatitis (3h). The apoptosis rate (number of activated caspase-3-positive cells in %) is significantly increased in exocrine cells of the pancreas of *Btc* and *Btc+Wa5* mice (n=4 males/group; age: 11 weeks), *: $P<0.05$.

2. Investigation of the role of ERBB4 in the development of the exocrine pancreas

2.1. Generation of conditional *Erbb4* knockout *(Erbb4-KO)* mice

To analyze the role of ERRB4 in the exocrine pancreas development and the AP, we generated animals carrying a homozygously floxed exon 2 within the *Erbb4* gene ($Erbb4^{flox/flox}$) and expressing in addition hemizygously Cre recombinase under the control of the *Pft1a* promoter ($Erbb4^{fl/fl}/Ptf1a/^{tm1(cre)Hnak}$).

2.1.1. Expression study

2.1.1.1. Validation of *Erbb4* deletion in the exocrine pancreas of the *Erbb4-KO* mouse by RT-PCR

RNA was isolated from several organs of control mice, expressing the murine wild type *Erbb4* sequence (*Erbb4*), and *Erbb4-KO* mice (male, aged 8 weeks) with the *Erbb4* sequence after conditional knockout under the control of *Ptf1a* promoter (*Erbb4-KO*). The RNA was reversely transcribed into cDNA which can be amplified by RT-PCR and separated by agarose gel electrophoresis. *Erbb4* expression could be confirmed in the heart, the kidney and the pancreas. A lower expression could be shown in the lung and no expression was found in the spleen

of wildtype mice. Due to a possible minimal *Ptf1a* activity in heart, lung, and kidney, these organs of *Erbb4-KO* mice showed also a minimal expression of the deleted *Erbb4* gene. The less intense band in the pancreas sample can be explained by the fast degradation of the pancreatic RNA due to autodigestion (Fig. 4.5).

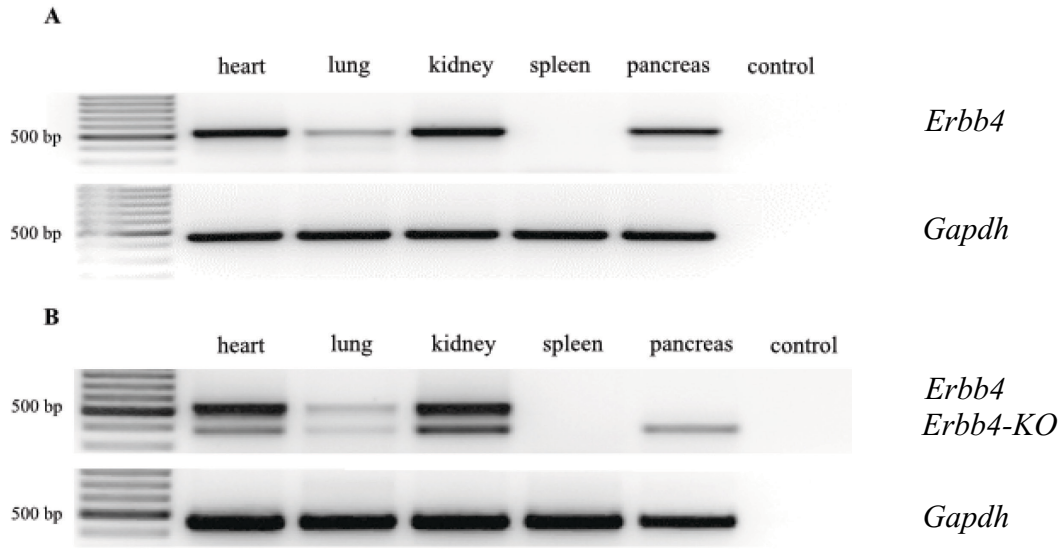

Figure 4.5: Expression pattern of murine wild type *Erbb4* (*Erbb4*) and *Erbb4* after conditional knockout under the control of the *Ptf1a* promoter (*Erbb4-KO*). *Erbb4* expression (531 bp) in heart, kidney and pancreas, lower expression in lung, no expression in spleen of wildtype mice (A). *Erbb4* and *Erbb4-KO* (lacking exon 2, length: 379 bp) expression in *Erbb4-KO* mice in heart, kidney and to a lower extend in the lung. The pancreas shows only expression of *Erbb4* lacking exon 2 (*Erbb4-KO*) (B). Bidistilled H_2O was used as negative control and *Gapdh* expression as standard.

2.1.1.2. Visualization of Cre by X-gal staining

To verify the activity of Cre in the exocrine pancreas, we crossbred *Ptf1a-Cre* mice with the reporter mouse line *Gt(ROSA)26Sor*$^{tm/Sor}$. *Gt(ROSA)26Sor*$^{tm/Sor}$ mice show an inducible ubiquitous expression of modified *LacZ* . Based on this *LacZ* expression, ß-galactosidase is expressed in cells with Cre activity, since Cre excises a stop cassette upstream of *LacZ*. ß-galactosidase activity can be visualized by X-gal staining. Cre was only expressed in the pancreas of *Ptf1a-Cre* mice, but not in other tissues. Fig. 4.6 shows an X-gal staining in the pancreas and in the kidney as an example.

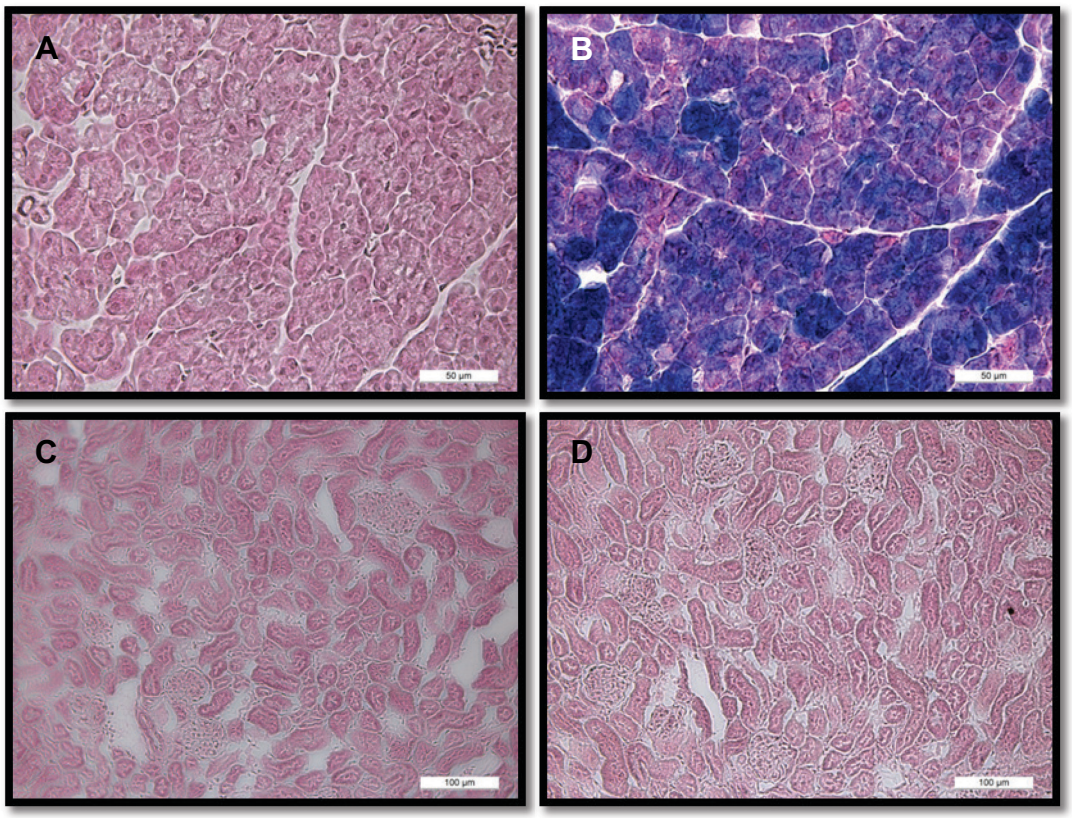

Figure 4.6: Examples of X-gal-stained pancreas (A, B) and kidney (C, D) of 8-week-old control (A, C) and *Ptf1a-Cre* +ROSA-lacZ mice (B, D) showing the specifity of the Cre enzyme in the exocrine pancreas. Scale bar represents 50 µm.

2.1.1.3. Detection of ERBB4 by immunohistochemical staining

The immunohistochemical staining demonstrated the expression of the ERBB4 receptor in the exocrine pancreatic tissue of the control but not in the exocrine pancreas of the *Erbb4-KO* mouse (Fig. 4.7).

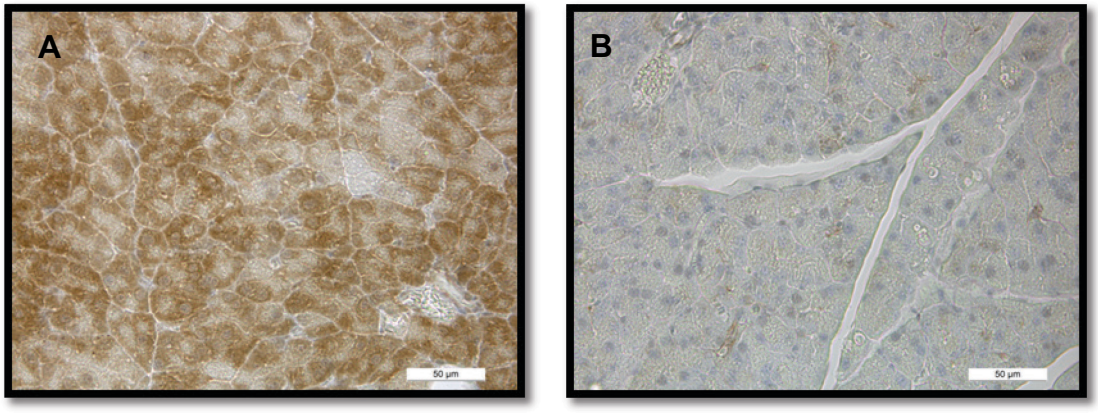

Figure 4.7: Immunoreactivity of ERBB4 in the exocrine pancreas of an 8-week-old male control (A) and *Erbb4-KO* mouse (B). The *Erbb4-KO* mouse shows almost no immunoreactivity for ERBB4. Scale bar represents 50 µm.

2.1.2. Body and organ weight analysis of *Erbb4-KO* mice

The body weights of *Erbb4-KO* mice and their wildtype littermates of both genders were recorded until the age of 12 weeks (Fig. 4.8). The loss of the ERBB4 receptor in the exocrine pancreas did not influence the body weight gain.

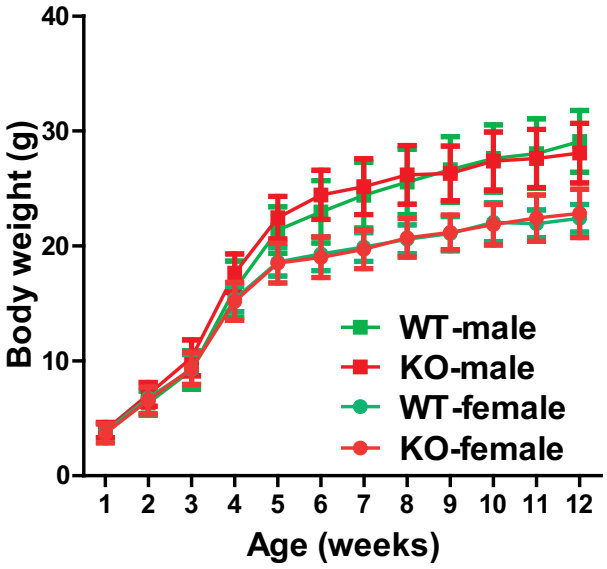

Figure 4.8: Postnatal growth curves of *Erbb4-KO* (KO) mice and their wildtype (WT) littermates (n =7) until the age of 12 weeks.

2.1.3. Exocrine pancreas

2.1.3.1. Evaluation of the pancreas weight of *Erbb4-KO* mice

The absolute pancreas weight and the pancreas weight in relation to the body weight were analyzed in 3-month-old and 1-year-old *Erbb4-KO* mice and their wildtype littermates, without revealing any effects based on the loss of ERBB4 (Fig. 4.9, Fig. 4.10).

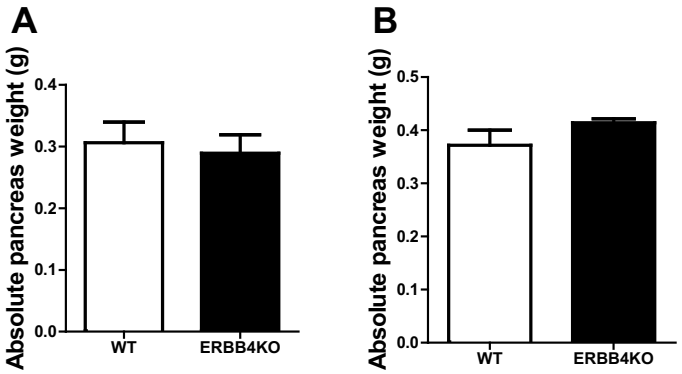

Figure 4.9: Absolute pancreas weights of male, 3-months-old (A) and 1-year-old female (B) *Erbb4-KO* mice and controls (n=4).

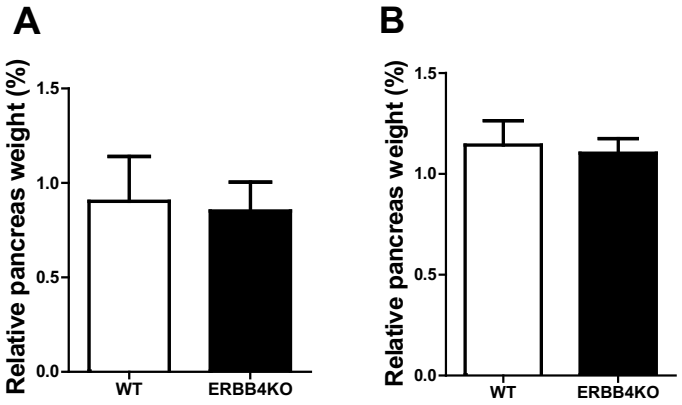

Figure 4.10: Relative pancreas weights of male, 3-months-old (A) and 1-year-old female (B) *Erbb4-KO* mice and controls (n=4).

2.1.3.2. Histology of the exocrine pancreas of *Erbb4-KO* mice

The pancreas of 3-month-old male *Erbb4-KO* knockout mice showed no obvious change in weight, size and constitution. Also in H&E-stained histological sections the pancreas did not show any structural changes (Fig. 4.11).

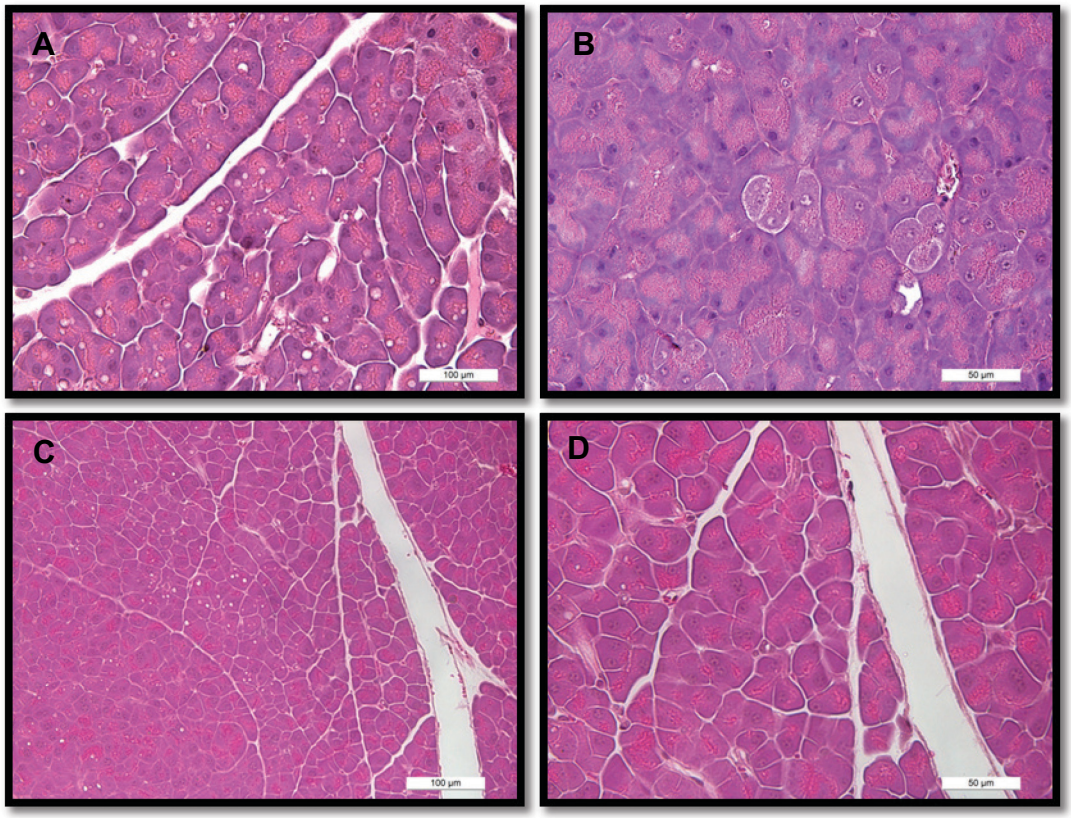

Figure 4.11: Examples of H&E-stained sections of the pancreas of 3-month-old male *Erbb4-KO* (A, B) and wildtype mice (C, D) in different magnifications. Scale bar represents 100 µm (A, C) and 50 µm (B, D).

3. Investigation of *Erbb4-KO* mice in caerulein-induced pancreatitis

3.1. Caerulein-induced pancreatitis

To analyze if the loss of the ERBB4 receptor influences AP, we applied the caerulein-induced pancreatitis model to wildtype and *Erbb4-KO* mice. For inducing the 24-hour-lasting pancreatitis we employed 5-month-old males. AP was induced by 8 injections of caerulein and the mice were killed 24 hours after the first injection. The mice were fasted for 18 hours before starting the experiment. The first serum markers of pancreatitis, serum amylase and lipase,

were measured in the two groups. No significant differences between wildtype and *Erbb4-KO* mice could be detected (Fig. 4.12).

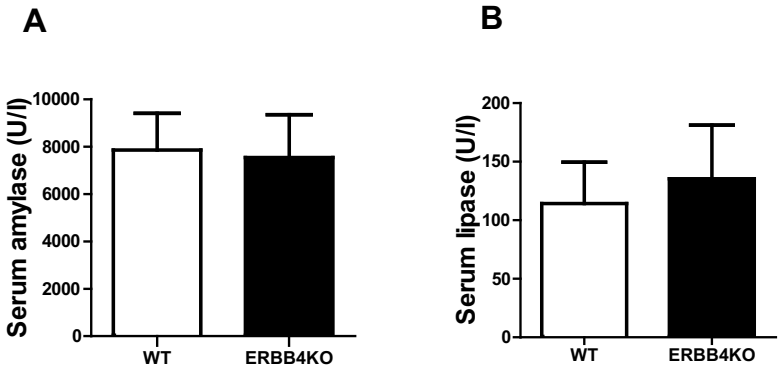

Figure 4.12: Serum amylase (A) and lipase (B) levels of 5-month-old male wildtype (WT) and *Erbb4-KO* (ERBB4KO) mice after a 24-hour-lasting, induced pancreatitis, (n=6/group).

The histological scoring was employed in the same way as described in chapter **1.2** to evaluate the severity of AP. 50 visual fields of H&E-stained pancreas per animal were examined without revealing any differences between wildtype and *Erbb4-KO* mice (Fig. 4.13 and Fig. 4.14).

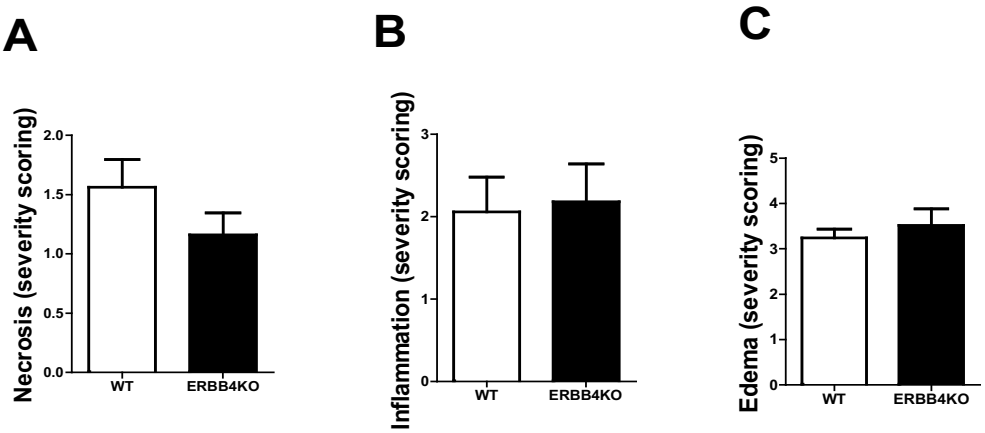

Figure 4.13: Histological scoring of caerulein-induced pancreatitis (24h) in 5-months-old male wildtype (WT) and *Erbb4-KO* mice (ERBB4-KO) evaluating the necrotic cells (A) the inflammation cells (B) and the edema (C), (n=6/group).

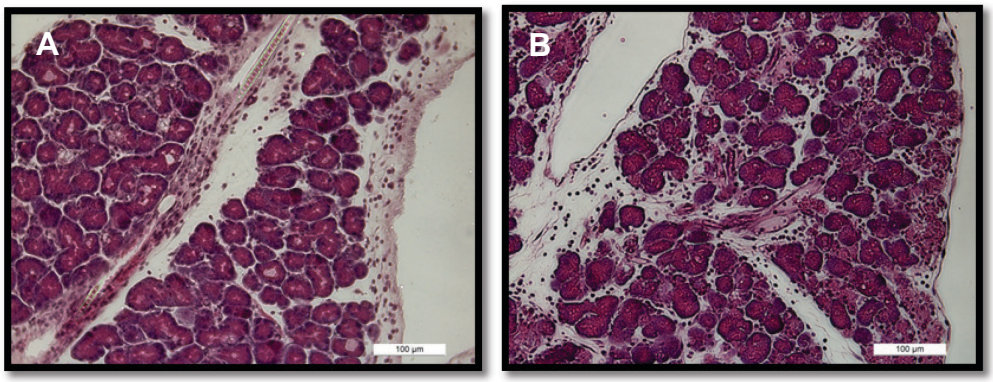

Figure 4.14: Examples of H&E-stained histological sections employed for the scoring of necrosis, inflammation and edema. Wildtype (A) and *Erbb4-KO* mice (B) show similar severity of AP. Scale bar represents 100 µm.

After the 24-hour-lasting pancreatitis the absolute and relative pancreas weight was measured. No differences between the two groups could be observed (Fig. 4.15).

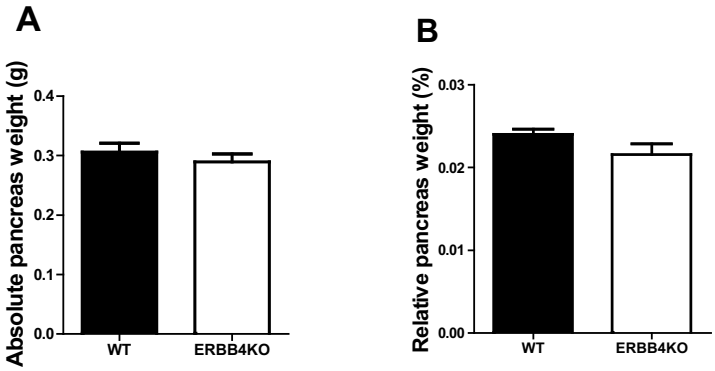

Figure 4.15: Absolute (A) and relative (B) pancreas weight of 5-month-old male *Erbb4-KO* compared to their wildtype (WT) littermates, after a 24-h-lasting induced pancreatitis (n=5/group).

3.2. Caerulein-induced pancreatitis followed by a regeneration period of 7 days

As the ERBB4 receptor seems to play a role in tissue regeneration in other organs, we induced a 24-hour-lasting pancreatitis with caerulein in male *Erbb4-KO* and wildtype mice. After the pancreatitis experiment the animals had a regeneration period of 7 days before they were sacrificed. Serum amylase and lipase were measured (Fig. 4.16) and the pancreas weight was documented without revealing

a significant difference between wildtype and knockout mice (Fig.4.17). The number of apoptotic cells and the proliferation rate were also assessed by using an apoptosis and proliferation index (Fig. 4.18). Again, no significant difference between the two animal groups could be detected.

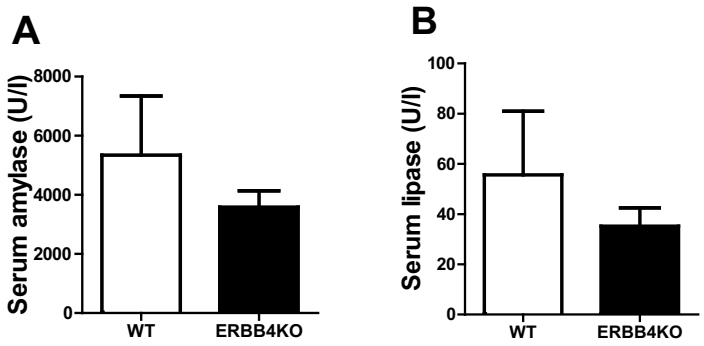

Figure 4.16: Serum amylase (A) and lipase (B) levels of 7-month-old male wildtype (WT) and *Erbb4-KO* mice after a 24-hour-lasting induced pancreatitis followed by a 7-day-lasting regeneration period (n=5/group).

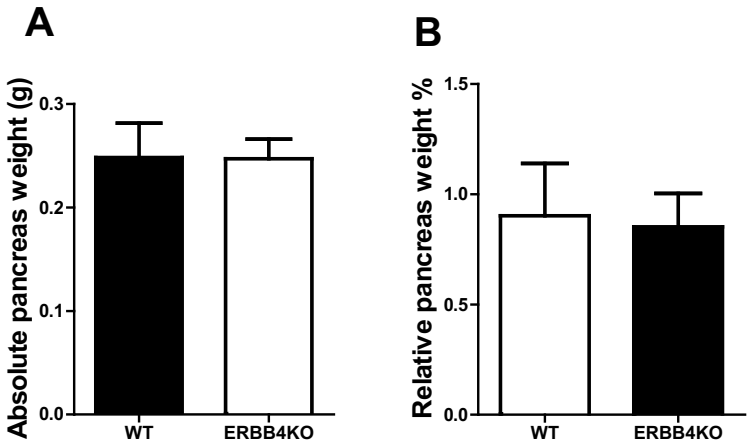

Figure 4.17: Absolute (A) and relative (B) pancreas weight of 7-month-old male wildtype (WT) and *Erbb4-KO* mice after the regeneration period of 7 days (n=5/group).

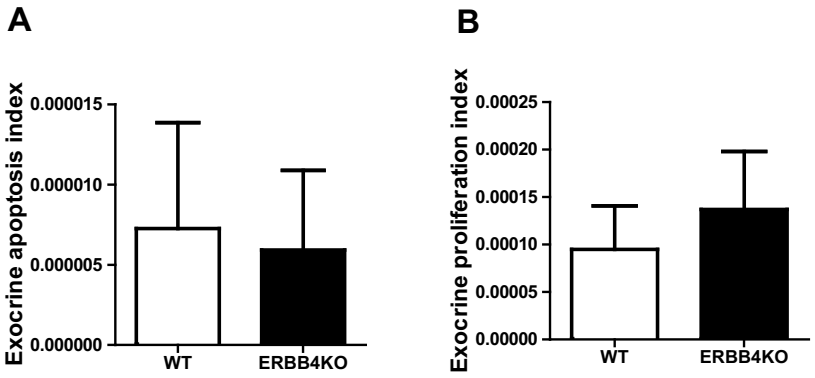

Figure 4.18: Apoptosis index (number of activated caspase-3-positive cells in % (A) and proliferation index (number of Ki67-positive cell nuclei in %) (B) of 7-month-old wildtype (WT) and *Erbb4-KO* mice after the induced pancreatitis (24h) and the subsequent regeneration period of 7 days, (n=4/group).

4. Investigations on the involvement of ERBB4 in mediating BTC effects in the exocrine pancreas

4.1. Generation of *Btc* transgenic mice in the *Erbb4* knockout background (*Btc+Erbb4-KO*)

To obtain mice with loss of ERBB4 in the exocrine pancreas and ubiquitous BTC-overexpression, we crossbred *Erbb4-KO* mice with *Btc* transgenic mice.

4.2. Body weight analysis of *Btc+Erbb4-KO* mice

In previous studies it has already been shown that *Btc* transgenic mice show reduced body weight gain. Wildtype littermates showed the same body weight as *Erbb4-KO* mice and *Btc* transgenic mice as *Btc+Erbb4-KO* (Fig. 4.19).

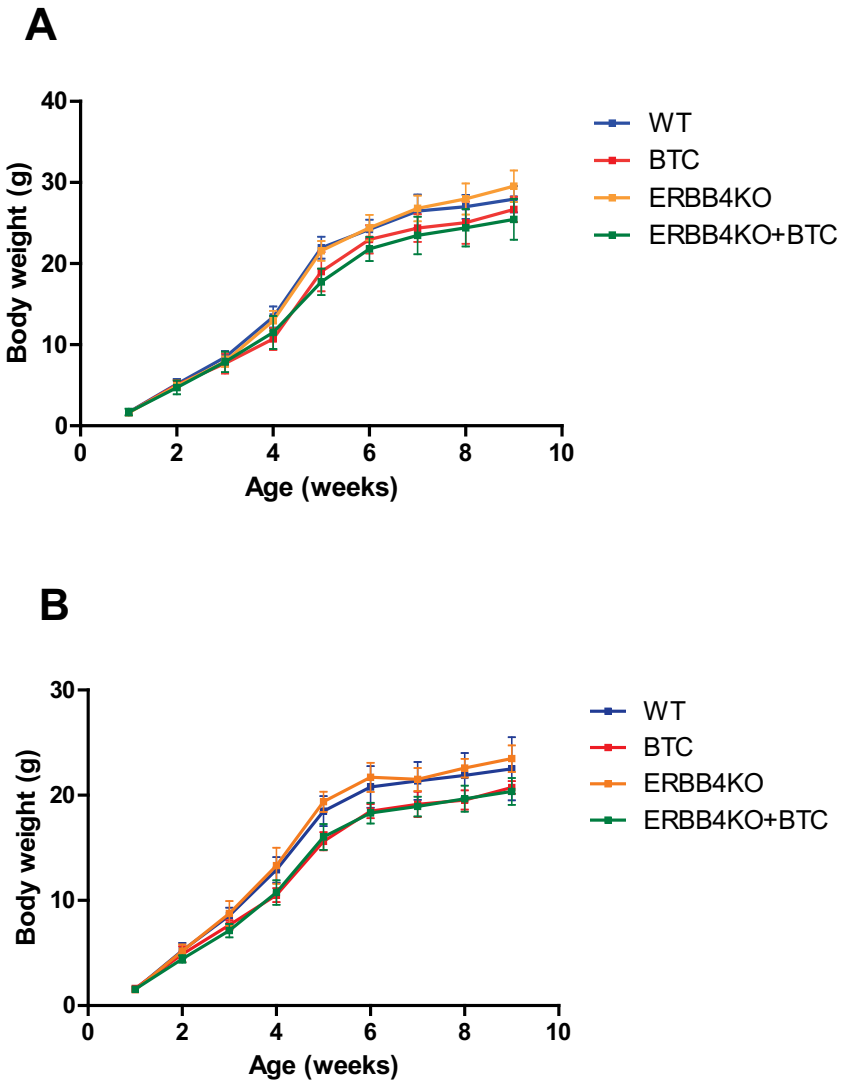

Figure 4.19: Postnatal growth curves of male (A) and female (B) *Btc+Erbb4-KO* (ERBB4KO+BTC) mice until the age of 9 weeks. As control groups we used wildtype (WT), *Btc* (BTC) and *Erbb4-KO* (ERBB4KO) littermates, (n=8/group).

4.3. Exocrine Pancreas

4.3.1. Evaluation of the pancreas weight of *Btc+Erbb4-KO* mice

It is already known that the pancreas weight of BTC-overexpressing mice is significantly reduced compared to wildtype littermates and that this effect is EGFR-independent. In previous studies we found out that the loss of ERBB4 does not influence the pancreas weight (chapter **2.1.3.1**). We compared the pancreas weight of male wildtype, *Erbb4-KO, Btc* transgenic and *Btc+Erbb4-KO* mice. The reduced pancreas weight in mice overexpressing BTC is not mediated by ERBB4 because *Btc+Erbb4-KO* mice continue to show reduced pancreas weight (Fig. 4.20).

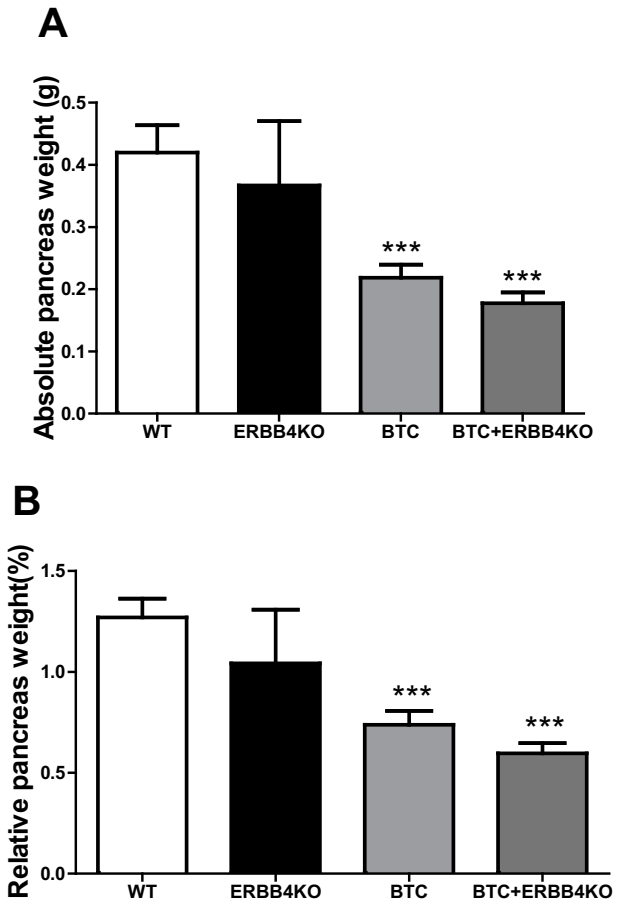

Figure 4.20: Absolute (A) and relative (B) pancreas weight of male wildtype (WT), *Erbb4-KO* (KO), *Btc* transgenic (BTC) and *Btc+Erbb4-KO* (BTC+ERBB4KO) mice, (n=4, 3 months), ***: $P<0.001$.

4.3.2. Histology of the pancreas

The pancreas of the four genotype groups (wildtype, *Erbb4-KO*, *Btc* and *Btc+Erbb4-KO*) at the age of 1 year was employed for histological analysis to assess whether the loss of ERRB4 influences the effect of BTC on the development of the exocrine pancreas. The absence of ERBB4 seems to activate a structural change of the acinar and duct cells of *Btc* transgenic mice (Fig. 4.21). These altered areas resemble lesions known as pancreatic intraepithelial neoplasia (PanIN) and show a higher number of BrdU-positive, proliferating cells (Fig. 4.22).

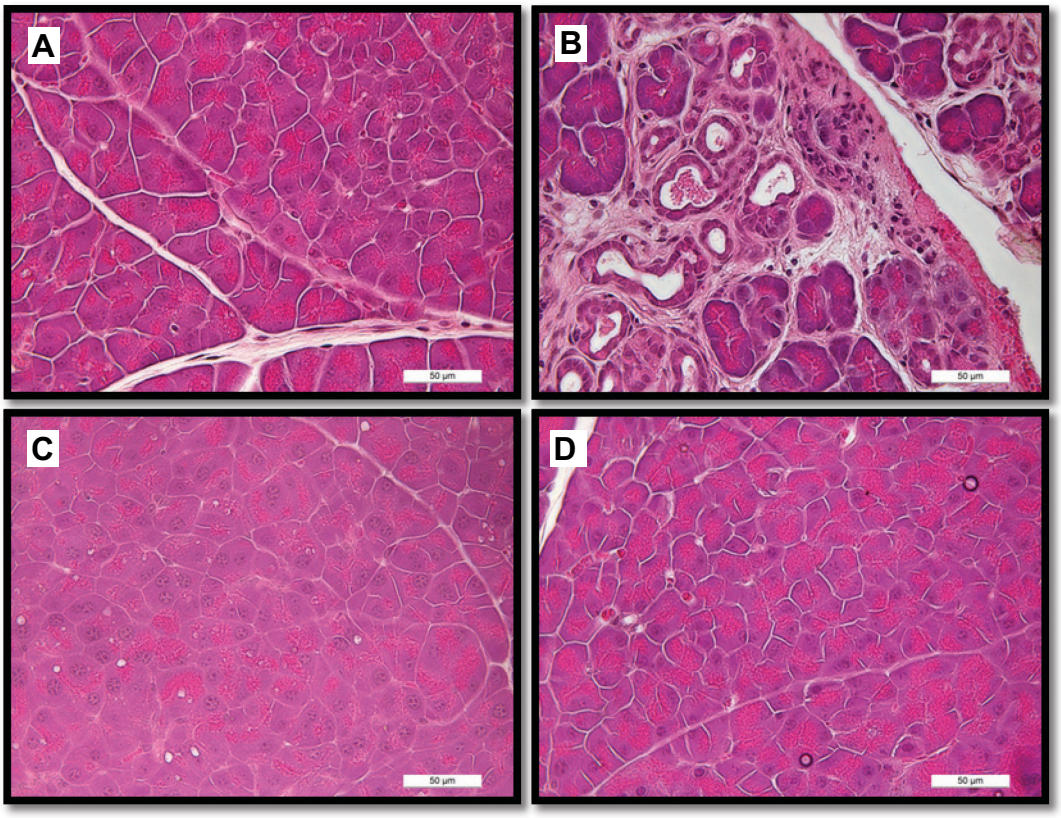

Figure 4.21: Examples of H&E-stained sections of the pancreas of 1-year-old *Btc* transgenic (A), *Btc+Erbb4-KO* (B), *Erbb4-KO* (C) and wildtype mice (D). Scale bar represents 50 µm.

BrdU-stained histological sections revealed that in the altered areas of the pancreatic tissue of *Btc+Erbb4-KO* mice a higher number of proliferating, BrdU positive nuclei could be detected (Fig. 4.22).

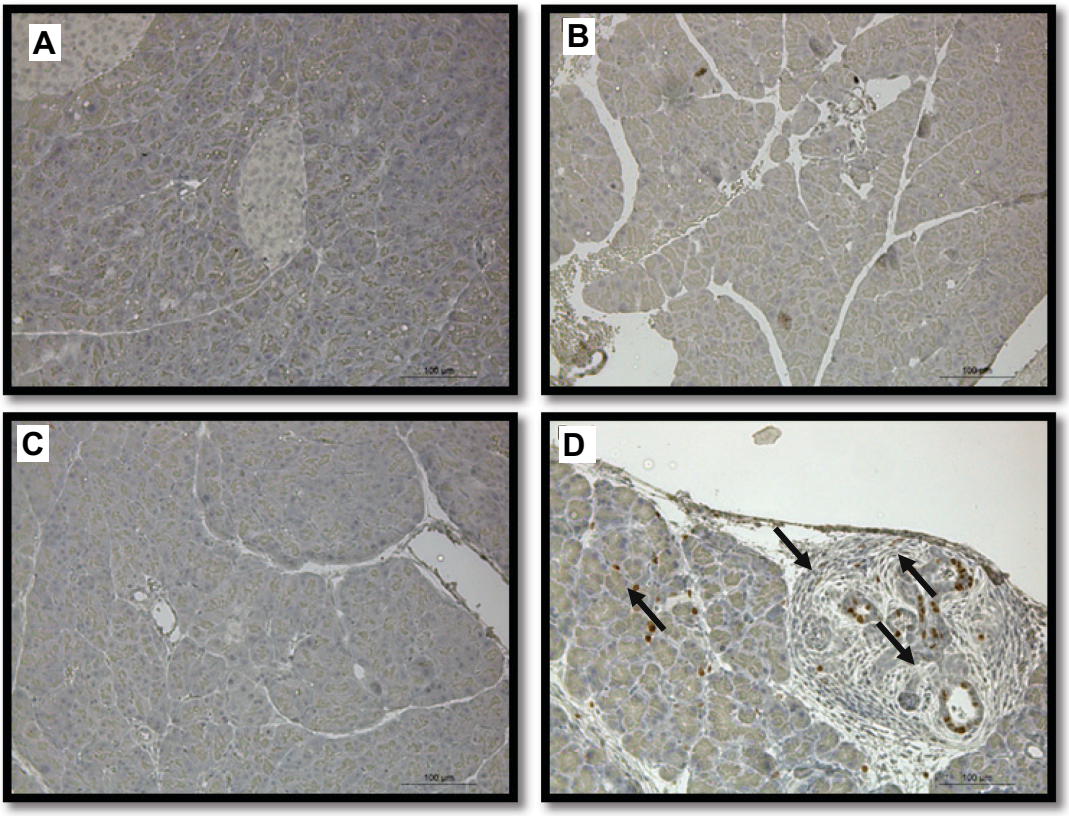

Figure 4.22: BrdU immunohistochemical labelling of 1-year-old wildtype (A), *Erbb4-KO* (B), *Btc* (C) and *Btc+Erbb4-KO* (D) mice. Scale bar represents 100 µm.

4.3.3. Acute pancreatitis

4.3.3.1. Caerulein-induced pancreatitis

A 24-hour-lasting pancreatitis was induced by 8 injections of caerulein and the female mice, aged 4 months, were killed 24 hours after the first injection. The mice were fasted for 18 hours before starting the experiment. The first serum markers of pancreatitis, serum amylase and lipase were measured in the four groups (Fig. 4.23). The analysis of serum after the 24-hour-lasting pancreatitis revealed that the *Btc+Erbb4-KO* mice showed similar values of amylase and lipase compared to *Erbb4-KO* and wildtype mice. Only *Btc* transgenic mice showed significantly reduced serum levels of amylase and lipase. Thus, the

protective effect of BTC is absent without the ERBB4 receptor and therefore mediated by ERBB4.

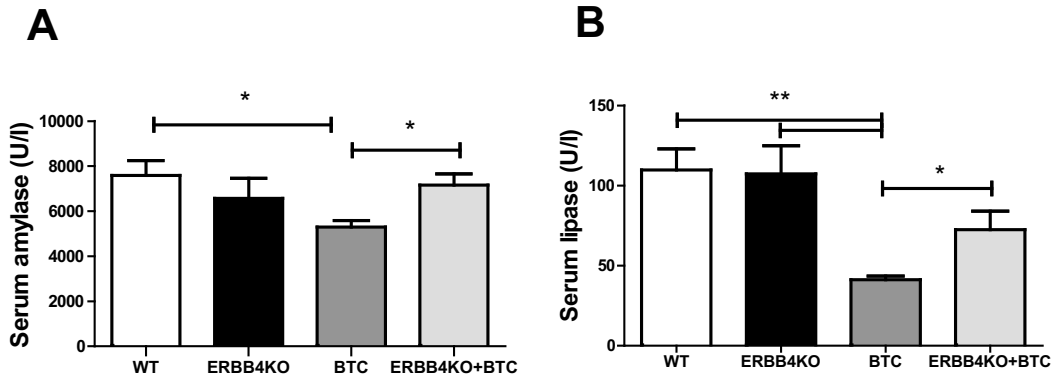

Figure 4.23: Serum amylase (A) and lipase (B) levels of the four animal groups (*Btc, Erbb4-KO, Btc+Erbb4-KO* and wt), (aged 4 months, female) after a 24-hour-lasting, induced pancreatitis (n=4/group), *: $P<0.05$. **: $P<0.01$.

The histological scoring was employed as in the chapters above (**1.2**) to evaluate the number of necrotic and inflammation cells and the grade of edema to estimate the severity of the induced pancreatitis. The *Btc* transgenic animals represented the only group with significantly decreased values in all categories compared to all other genotypes where the pancreatitis was manifested with its typical features. Thus, without the ERBB4 receptor, the protective effect of BTC is no longer present (Fig. 4.24 and Fig. 4.25).

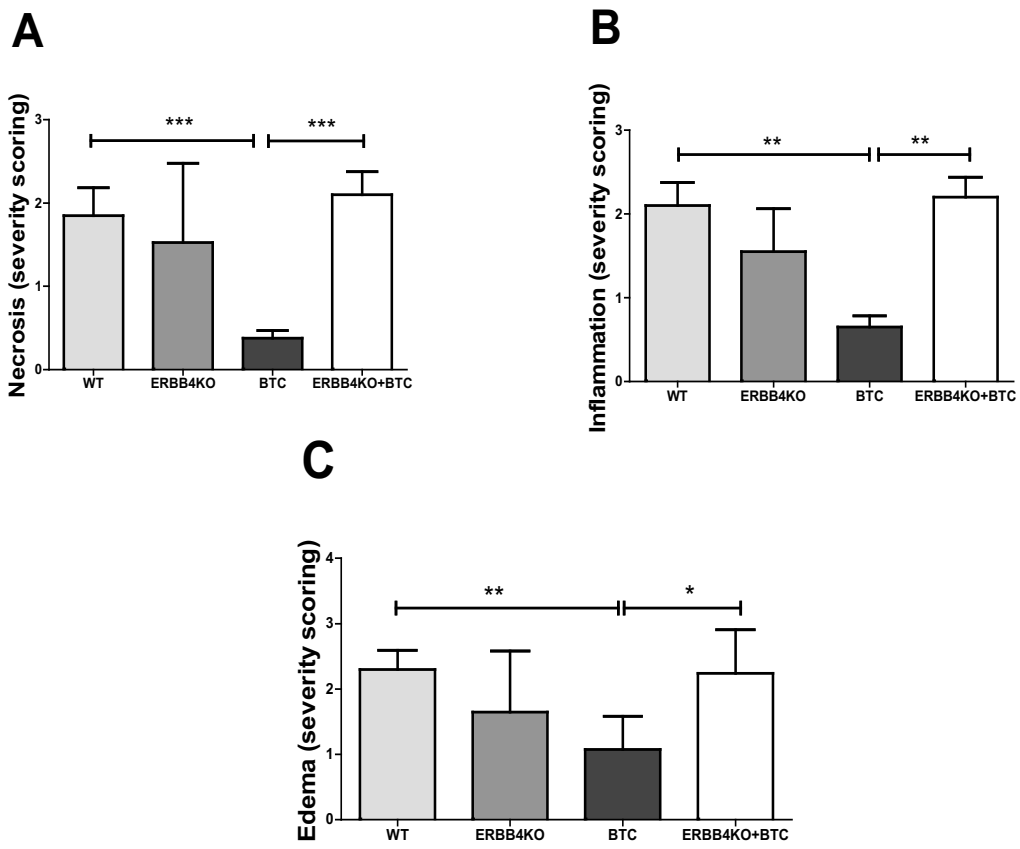

Figure 4.24: Histological scoring of the caerulein-induced pancreatitis (24h) evaluating necrotic cells (A) inflammation cells (B) and edema (C). *Btc+Erbb4-KO* mice compared with the respective animal groups (n=5/group), (females, aged 4 months) *: $P<0.05$, **: $P<0.01$, ***: $P<0.001$.

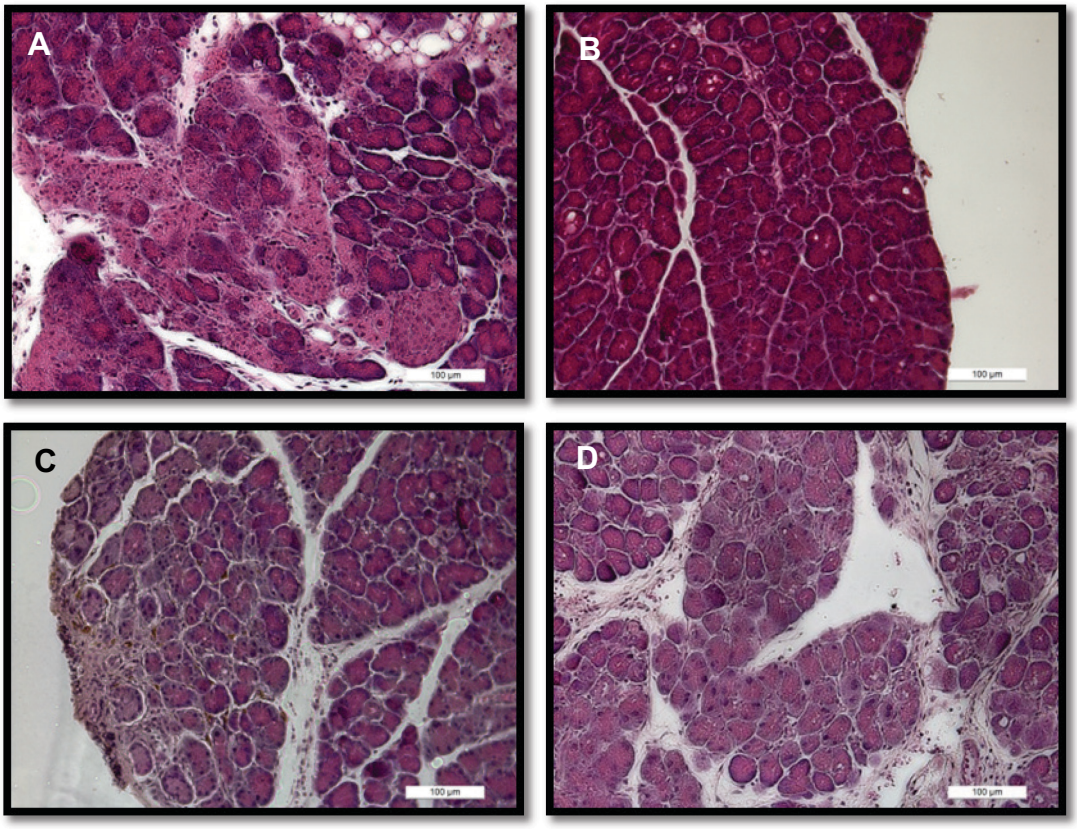

Figure 4.25: Examples of H&E-stained histological sections employed for the scoring of necrosis, inflammation and edema. Wildtype (A), *Btc+Erbb4-KO* mice (D) and *Erbb4-KO* mice (C) show the main indications of AP with invasion of inflammation cells, necrosis and edema (3 months-old females). Only the *Btc* transgenic mice (B) are protected. Scale bar represents 100 µm.

4.3.3.2. Pancreatitis model induced by L-arginine

To ensure that the results of the caerulein-induced pancreatitis can be reproduced in other pancreatitis experiments, we applied the L-arginine pancreatitis model to male *Btc+Erbb4-KO* mice. The mice received food *ad libitum*. The L-arginine pancreatitis was induced by 2 hourly injections of L-arginine (4 g/kg). Blood was collected 0, 24, 48, and 72 hours after the first injection. After that, the mice were sacrificed and tissue samples were removed. Serum amylase was measured in the four groups. The chemical analysis of serum after 0, 24, 48 and 72 hours revealed that the *Erbb4-KO* mice with additional BTC-overexpression showed similar values of amylase and lipase as *Erbb4-KO* and wildtype mice (Fig 4.26). Thus, the pancreatitis induced by L-arginine showed results similar to those in the

pancreatitis model induced by caerulein.

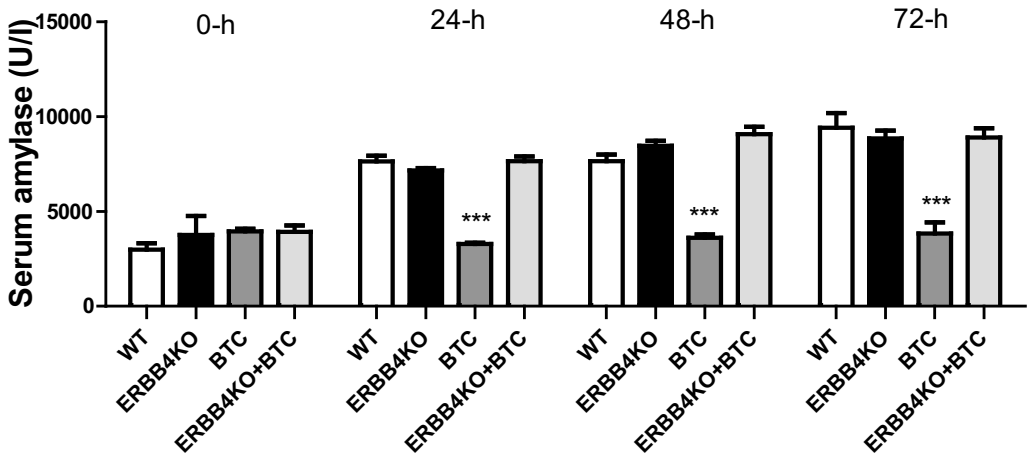

Figure 4.26: Serum amylase levels of the four groups (*Btc, Erbb4-KO, Btc+Erbb4-KO* and wt), after a 24-hour-lasting, induced pancreatitis (aged 6 months, males). After 24 hours, 48 hours and after 72 hours only the *Btc* transgenic mice are protected and show significantly decreased amylase levels in the serum (n=4/group), *: $P<0.05$, **: $P<0.01$

The histological scoring was performed as in the caerulein-induced pancreatitis model. The *Btc* transgenic showed significantly decreased values in all categories compared to wildtype, *Erbb4-KO* and *Btc+Erbb4-KO* animals, in which the pancreatitis was manifested with its typical features. Thus, the loss of the ERBB4 receptor in the exocrine pancreas leads to the loss of protection by BTC (Fig. 4.27 and Fig. 4.28).

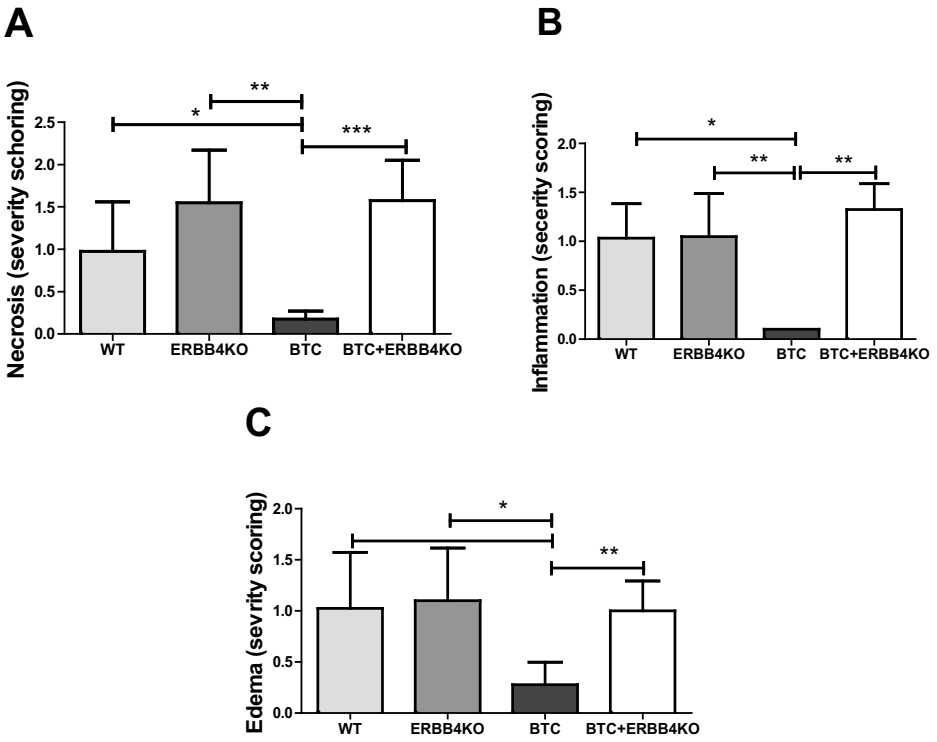

Figure 4.27: Histological scoring of 6-month-old male *Btc+Erbb4-KO* mice (BTC+ERBB4KO) and the respective control groups (WT, ERBB4KO and BTC) evaluating the necrotic cells (A) the inflammation cells (B) and the edema (C), (n=4/group), *: $P<0.05$, **: $P<0.01$, ***: $P<0.001$.

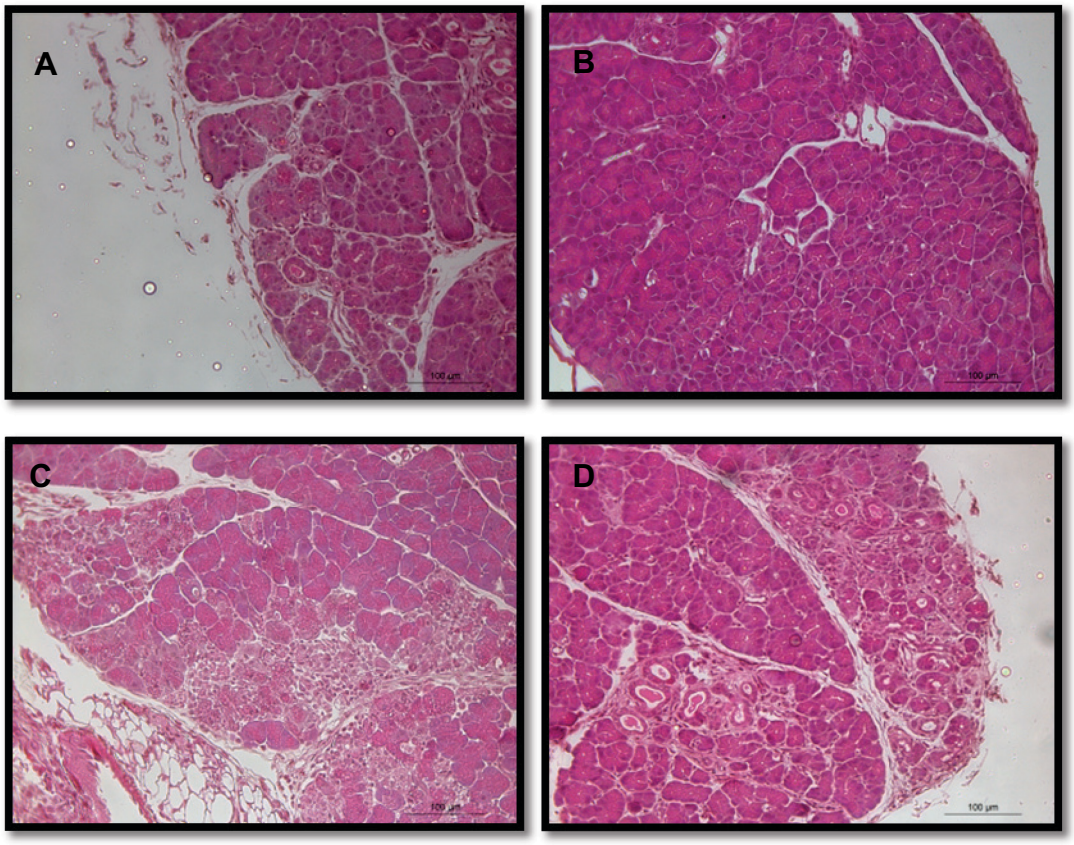

Figure 4.28: Examples of H&E-stained histological sections employed for the scoring of necrosis, inflammation and edema. Wildtype (A), *Btc+Erbb4-KO* mice (D) and *Erbb4-KO* mice (C), (aged 6 months, male) show the main indications of AP with immigration of inflammation cells, necrosis and edema. Only the *Btc* transgenic mice (B) are protected. Scale bar represents 100 µm.

5. Pathways activated by BTC signalling mediating the protection against AP

The only signalling cascade mediated by BTC that is known to be relevant for the protective effect in AP is the stress activated protein kinase (SAPK) pathway. The main pathways activated by the ERBB receptors are the MAPK (mitogen activated protein kinase) and AKT/PKB (3-kinase activated protein kinase B) pathways. It is also known that the cytoplasmatic tail of the ERBB4 receptor can be shaded by a γ-secretase and translocate to the nucleus where it can act as transcription factor.

5.1. SAPK signalling

To confirm an increased activation of the SAPK by BTC, a Western blot analysis was performed for phosphorylated SAPK and total SAPK (Fig. 4.29). Samples from male wildtype, *Btc* transgenic mice, *Btc+Erbb4-KO* and *Erbb4-KO* mice subjected to caerulein-induced 3-h-lasting pancreatitis were investigated by Western blot analysis. Phosphorylated SAPK is increased in the pancreas of BTC transgenic mice but not in the pancreas of BTC transgenic mice with additional deletion of ERBB4. These results suggest an activation of the SAPK pathway via BTC with an involvement of ERBB4.

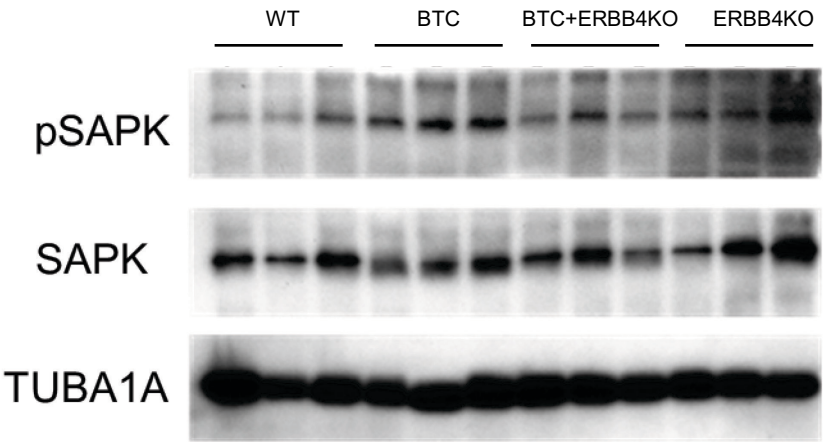

Figure 4.29: Western blot analysis of SAPK and pSAPK in pancreatic tissue of *Btc* transgenic (BTC), wildtype (WT), *Btc+Erbb4-KO* (ERBB4-KO+BTC) and *Erbb4-KO* (ERBB4-KO) mice, (male, 3 months) with acute 3-hour-lasting pancreatitis. α–tubulin (TUBA1A) was used as loading control.

5.2. MAPK signalling

To detect the activation of MAPK by BTC a Western blot analysis was performed for phosphorylated MAPK and total MAPK (Fig. 4.30). Caerulein-induced 3-h-lasting pancreatitis activated MAPK signalling, as demonstrated by the increased phosphorylation of MAPK. There was no difference in total MAPK detection or in the detection of its phosphorylated form in BTC-overexpressing mice compared to the wildtype mice in both groups (with and without 3-h-lasting pancreatitis). Thus, AP induces MAPK signalling, whereas BTC-overexpression has no effect on MAPK signalling.

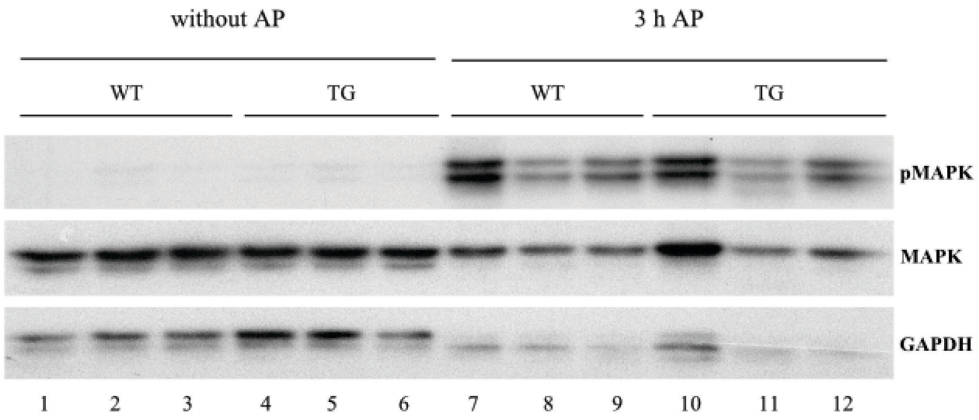

Figure 4.30: Western blot analysis of MAPK signalling in pancreatic tissue of male *Btc* transgenic (TG) and wild type mice (WT) with acute 3-hour-lasting pancreatitis (1-6) compared to healthy littermates (7-12), (male, 3 months). GAPDH was used as loading control.

5.3. AKT signalling

AKT/PKB is frequently involved in apoptotic pathways. We detected total AKT and the phosphorylated form of AKT in Western blot analysis. Western blot analysis revealed no alterations in AKT signalling in both animal groups (male, 3 months), indicating that BTC does not activate the AKT pathway in AP (Fig. 4.31).

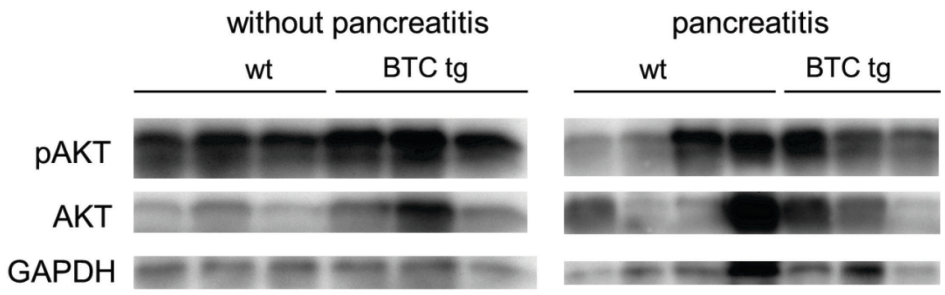

Figure 4.31: Western blot analysis of AKT signalling in pancreatic tissue of *Btc* transgenic (BTC tg) and wild type (wt) mice with and without 3-hour-lasting pancreatitis induced by caerulein (male, 3 months). GAPDH was used as loading control.

5.4. Nuclear localization of ERBB4 in pancreatic tissue

We performed a protein fractionation of pancreatic tissue to confirm the migration of ERBB4 and its intracellular domain (ICD) into the nucleus. Pancreatic tissue of wildtype and *Btc* transgenic animals was fractionated in its subcellular components (membrane, cytoplasm and nucleus).

5.4.1. Control of fractionation of pancreatic tissue

To confirm the success of the fractionation, Western blot analysis using antibodies detecting specific subcellular components were carried out: GAPDH for the cytoplasmatic fraction, ERBB2 for the membrane fraction, and Histone H3 for the nuclear fraction (Fig. 4.32).

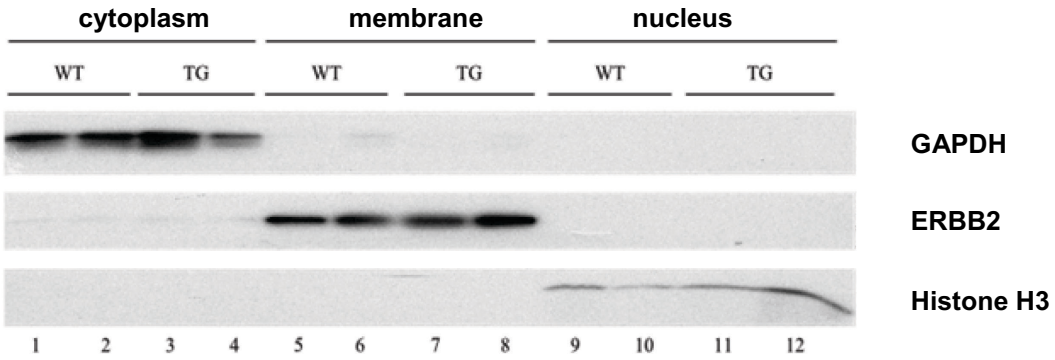

Figure 4.32: Western blot analysis as control of pancreatic tissue fractionation. The indicated proteins can be detected exclusively in their appropriate cell compartment. Cytoplasmatic fraction (1-4), membranous fraction (5-8), nuclear fraction (9-12), the first two lanes are wild type (WT), the last two lanes *Btc* transgene (TG) samples.

5.4.2. Subcellular ERBB4 detection in pancreatic tissue

To localize the ERBB4 receptor and its intracellular domain (ICD), the fractions were separated by SDS-PAGE and blotted onto a PVDF membrane. Pancreas samples of 3-month-old, male *Btc* transgenic animals and wild type littermates were used.

Even in control mice the ERBB4 receptor was not exclusively found in the membrane as expected, but also in the cytoplasmic fraction and in the nucleus. Whereas the level of ERBB4 remained constant in the membrane of BTC-overexpressing mice a significant increase of ERBB4 could be observed in cytoplasmic and nuclear fractions (Fig. 4.33, A).

The 120 kDa ICD of the ERBB4 receptor was not detectable in the membranous fraction of the pancreatic tissue, neither in the wild type, nor in the transgenic samples. In wildtype mice the soluble ICD could be distinctly detected in the

cytoplasm even in control mice. However, the amount of ICD increased in the cytoplasm in the pancreas sample of BTC-overexpressing mice compared to the wildtype mice or to the control (wildtype heart). In wildtype samples no ICD could be detected in the nucleus. However, small amounts of ICD could be detected in the nucleus of tissue samples of BTC-overexpressing mice, indicating a successful translocation of the soluble ICD to the nucleus upon BTC binding (Fig. 4.33, B).

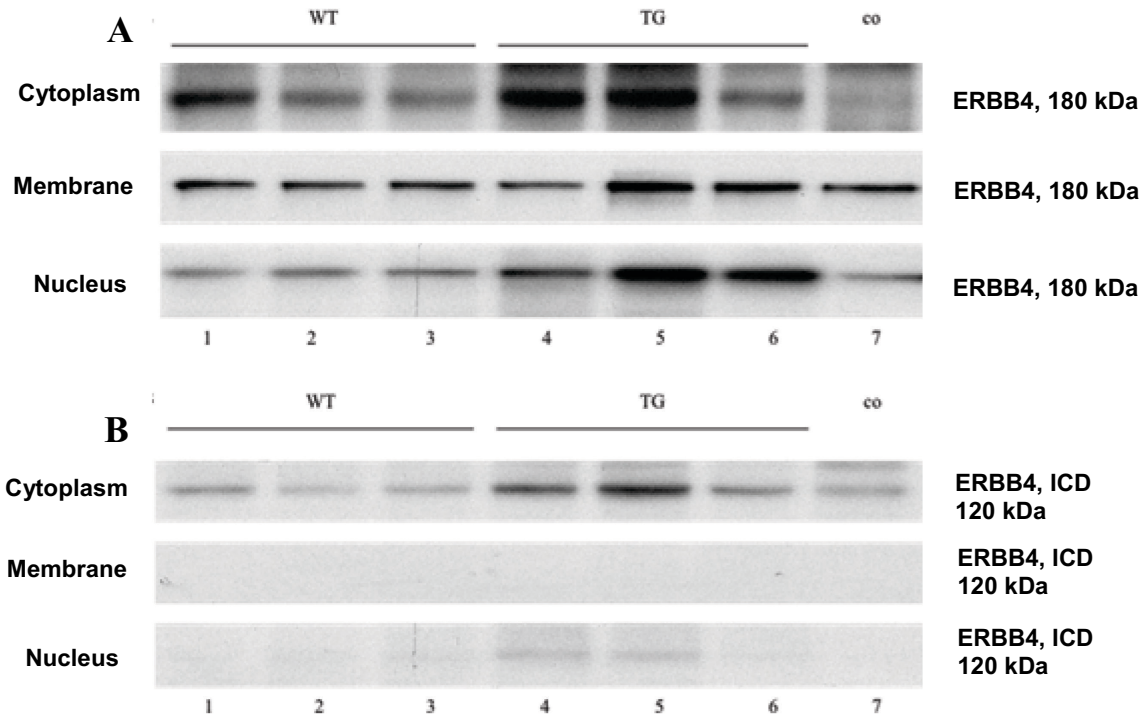

Figure 4.33: Western blot analysis and detection of ERBB4 (A) and its ICD (intracellular domain) (B) in subcellular compartments after fractionation of pancreatic tissue of wildtype (WT, 1-3) and *Btc* transgenic (TG, 4-6) mice (male, aged 3months). As positive control the subcellular compartments of heart tissue of wildtype mice was used (7).

5.5. Upregulated genes in *Btc* transgenic mice with and without AP

5.5.1. Microarray analysis

To find out which genes, activated by BTC via ERBB4 could be important for the protection against AP by BTC, pancreas samples of 9-week-old male *Btc* transgenic mice and controls, with and without AP (3h) were evaluated by microarray analysis. **Table 3** shows the genes significantly upregulated in transgenic animals with 0h- and 3h-pancreatitis compared with 0h- and 3h-pancreatitis control littermates. Genes only regulated in transgenic animals with 3h-pancreatitis compared with control animals with 3h-pancreatitis are shown in **Table 4**.

Table 3: Genes significantly (P<0.05) upregulated in pancreas samples of *Btc* transgenic animals (male, aged 9 weeks) at time points of 0h- and 3h-pancreatitis, (n=5/group). Yellow marked genes were subsequently measured by qRT-PCR.

PROBE SET ID	FC (LOG2)	P-VALUE	ID-NUMBER	GENNAME
A_55_P2178036	6.08	0.00001	NM_007618	Serine peptidase inhibitor, clade A, member 6
A_51_P133562	5.92	0.00001	NM_007618	Serine peptidase inhibitor, clade A, member 6
A_66_P118635	3.24	0.00023	ENSMUST00000095451	Gm46
A_51_P160713	5.01	0.00023	NM_009654	Albumin
A_51_P426270	2.38	0.00031	NM_008597	Matrix Gla protein
A_55_P2050902	3.67	0.00031	NM_021564	Fetuin beta
A_55_P2017939	1.84	0.00034	NM_011836	Laminin gamma 3

Table 4: Genes significantly (P<0.05) upregulated in pancreas samples of *Btc* transgenic mice (male, aged 9 weeks) in 3h-pancreatitis only, (n=5/group). Yellow marked genes were subsequently measured by qRT-PCR.

PROBE SET ID	FC (LOG2)	P-VALUE	ID-NUMBER	GENNAME
A_55_P1967548	2.38	0.00001	ENSMUST0000010611	GM6370
A_55_P1973159	1.86	0.00100	NM_011340	Serine peptidase inhibitor, clade F, member 1
A_55_P2207255	1.44	0.00288	NM_016911	Sushi-repeat-containing protein
A_55_P2035946	2.00	0.00288	NM_001002927	Preproenkephalin
A_51_P341736	1.92	0.00288	NM_008610	Matrix metallopeptidase 2
A_55_P1954086	3.01	0.00650	NM_001198766	Periostin, osteoblast specific factor
A_52_P14456	1.95	0.00650	NM_026886	Serine/arginine repetitive matrix 4
A_51_P167527	2.48	0.00857	NM_008524	Lumican
A_51_P157042	1.13	0.01031	NM_010217	Connective tissue growth factor
A_51_P255699	1.53	0.01031	NM_010809	Matrix metallopeptidase 3
A_51_P283473	1.64	0.01031	NM_026271	Fin bud initiation factor homolog (zebrafish)
A_55_P2149951	1.42	0.01591	NM_019412	Periaxin
A_55_P1968488	2.39	0.02395	NM_008118	Gastric intrinsic factor
A_52_P437795	1.81	0.02611	NM_009866	Cadherin 11
A_55_P2064328	1.56	0.02611	NM_008481	Laminin, alpha 2
A_51_P182303	1.89	0.02611	NM_007743	Collagen, type I, alpha 2
A_55_P2020577	1.68	0.02716	NM_008788	Procollagen C-endopeptidase enhancer protein
A_55_P1952618	1.39	0.03182	NM_007895	Eosinophil-associated,ribonuclease A family,member 2
A_55_P2130178	1.72	0.03182	NM_010233	Fibronectin 1
A_55_P2035662	1.38	0.03182	NM_009636	AE binding protein 1
A_55_P2142028	1.42	0.03391	NM_030179	CAP-GLY domain containing linker protein family
A_55_P2118520	2.47	0.04088	NM_007742	Collagen, type I, alpha 1
A_55_P2128853	1.37	0.04125	NM_001012766	Eosinophil-associated,ribonuclease A family,member 12
A_51_P146633	0.99	0.04369	ENSMUST00000143791	bicaudal C homolog 1

Based on a literature research *Cbg (Serpina6)*, *Pedf (Serpinf1)*, *Penk* and with less probability *Mmp2* and *Mmp3,* could play a role in AP and might be responsible for the protective effect of BTC.

5.5.2. qRT-PCR study of *Cbg*, *Pedf*, *Mmp2* and *3* and *Penk*

To confirm the results of the microarray study, a quantitative real-time PCR was employed. cDNA samples of 9-week-old, male *Btc* transgenic and control mice with AP (3h) were used. All investigated genes were significantly increased in *Btc* transgenic mice at RNA level (Fig.4.34)

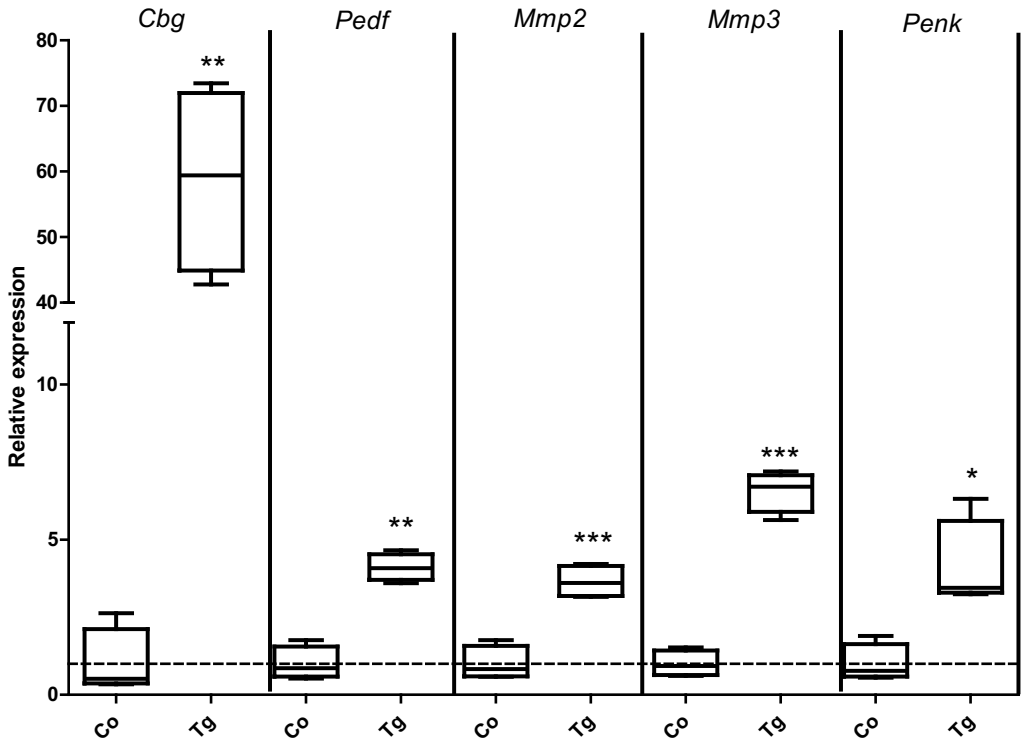

Figure 4.34: Quantitative RT-PCR analysis of the expression of *Cbg*, *Pedf*, *Mmp2* and *Mmp3* and *Penk* in pancreatic tissue of *Btc* transgenic mice (Tg) and controls (Co) with a 3-h-lasting pancreatitis, (n=5/group), (male, aged 9 weeks), *: $P<0.05$, **: $P<0.01$, ***: $P<0.001$.

5.6. CBG and PEDF protein expression analysis

CBG and PEDF were investigated in Western blot analysis using pancreas samples of wildtype and *Btc* transgenic mice (male, 8 weeks) with and without AP (3h) (Fig. 4.35). The Western blot analysis validated the upregulation of CBG in *Btc* transgenic mice. The protein could be detected in the pancreas of BTC-overexpressing mice to a higher level than in the controls. The results of the Western blot analysis confirmed the involvement of CBG in BTC signalling. The Western blot analysis of PEDF confirmed its upregulation in AP in both animal groups. However, there is no difference between *Btc* transgenic mice and the

control group. This data suggest that PEDF might play a role in AP, but not in BTC signalling.

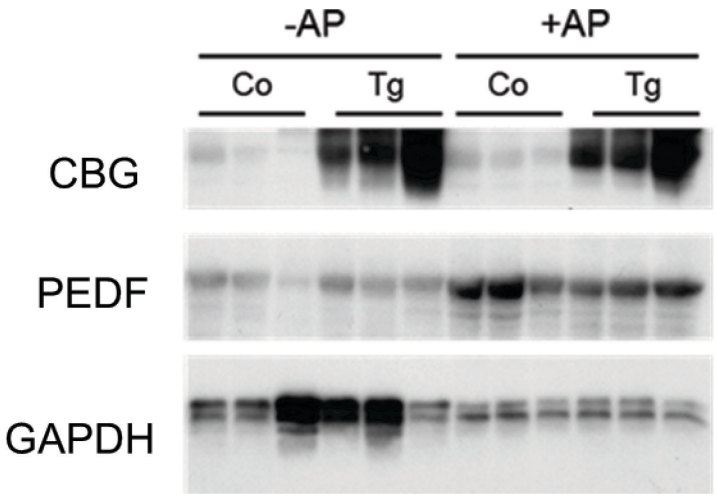

Figure 4.35: Western blot analysis of CBG and PEDF in pancreatic tissue of *Btc* transgenic (Tg) and wildtype (Co) mice (male, 8 weeks) with acute 3-hour-lasting pancreatitis (AP) compared to healthy littermates. GAPDH was used as loading control.

V. DISCUSSION

1. BTC-induced protection against AP requires normal EGFR activity

Previous studies describing the dominant expression of ERBB4 in the exocrine pancreas, and the fact that the reduced pancreas weight of *Btc* transgenic mice is not mediated by the EGFR, suggested that the protective effect of BTC against AP is ERBB4 dependent (Dahlhoff, 2010). Our results from the pancreatitis experiment employing mice without functional EGF receptor and additional ubiquitous BTC-overexpression validated this assumption since these animals were further on protected against AP. Nevertheless, as the *Wa5* mouse shows a residual activity of the EGF receptor (Lee, 2004) it cannot be fully excluded that the protection could be mediated by this residual receptor activity.

2. Loss of pancreatic ERBB4 does not affect mouse development and growth

To find out more about the role of pancreatic ERBB4, and in special whether the loss of ERBB4 in the pancreas can affect mouse development and growth, we investigated conditional *Erbb4-KO* mice, which are deficient for ERBB4 in the exocrine pancreas. The pubs were viable and showed no conspicuities compared to their wildtype littermates. Because mice with ubiquitous ERBB4 deletion die between day 10 and 11 after fertilization (Gassmann, 1995), it was not predictable if the loss of ERBB4 in the exocrine pancreas would be compatible with normal development and the birth of viable pubs. As no differences regarding the body weight gain compared to wildtype littermates could be detected, our data indicate that ERBB4 expression in the exocrine pancreas is not important for normal mouse development.

ERBB receptors are known to play an important role in cell differentiation and development (Massague, 1993), (Holbro, 2003). Surprisingly, the loss of ERBB4 has no influence on normal pancreatic development. The pancreas of *Erbb4-KO* mice showed no macroscopic alterations and even in H&E stained histological

sections we could not observe any changes in cell structure or general constitution.

In case of additional BTC-overexpression, the implications of ERBB4 loss seem to be more complex. In *Erbb4-KO* mice with additional BTC-overexpression the body weight is only influenced by the overexpressed BTC as established in previous studies (Schneider, 2005). The body weight analysis revealed that *Btc* transgenic mice as well as the *Erbb4-KO* mice with additional BTC-overexpression showed a significantly reduced body weight gain compared to wildtype littermates and *Erbb4-KO* mice. That implies that *Erbb4-KO* mice behave like wildtype mice and *Erbb4-KO* mice with additional BTC overexpression like *Btc* transgenic mice, demonstrating that the pancreatic ERBB4 receptor does not mediate the reduced body weight in *Btc* transgenic mice. One explanation for an impaired body weight gain of *Btc+Erbb4-KO* mice could result from morphologic changes in the exocrine pancreatic tissue, affecting the ability to store and synthesize the necessary amount of digestive enzymes.

The pancreas weight of *Erbb4-KO* mice with additional BTC-overexpression and in *Btc* transgenic mice is significantly reduced compared to wildtype mice and *Erbb4-KO* mice. According to these results, the ERBB4 receptor is not responsible for the reduced pancreas weight caused by overexpressed BTC. This implies that another ERBB receptor or a combination of different receptors has to be responsible for this effect.

Interestingly, in H&E and BrdU stained histological pancreatic sections of 1-year-old *Erbb4-KO* mice with additional BTC-overexpression, structural changes in the acinus and duct cells, resembling lesions known as pancreatic intraepithelial neoplasia (PanIN) were apparent. As a further evidence for a neoplastic alteration these areas showed a higher number of BrdU positive, proliferating cells. Considering the complexity of the ERBB system with its different pathways, it seems possible that the overexpressed BTC is able to bind and activate different hetero- or homodimers of the ERBB receptor family even without its binding partner ERBB4. The ERBB2/3 heterodimer is known to be involved in carcinogenesis (Pinkas-Kramarski, 1998) and could therefore be responsible for these alterations in the pancreatic tissue. Notably, BTC is able to activate several heterodimers of ERBB receptors, including the ERBB2/3 heterodimer (Alimandi, 1997), (Pinkas-Kramarski, 1998).

3. Role of ERBB4 in AP with or without BTC-overexpression

Even if the loss of pancreatic ERBB4 does not affect pancreatic development, it is possible that *Erbb4-KO* mice show an altered course of AP. ERBB4 is known to play a role in inflammation processes such as lung inflammation (Purevdorj, 2008) and Crohn's colitis (Frey, 2009) by mediating proaptotic pathways (Sartor, 2001), (Vidal, 2005). This activation of proapoptotic pathways might lead to a higher apoptosis rate and thus protection against AP. However, these findings could not be validated in our AP experiments where *Erbb4-KO* mice behaved like wildtype mice. Consequently, the loss of ERBB4 itself does not affect the course and severity of AP.

We also found out that the loss of ERBB4 does not influence the capability of the pancreatic tissue to regenerate after induced AP. *Erbb4-KO* mice suffering from induced 24-h-lasting pancreatitis, followed by a regeneration period of 7 days, did not show any evidences of reduced cell regeneration. In this case, ERBB4 does not seem to mediate pathways responsible for cell regeneration and survival, as suggested in previous studies (Frey, 2009).

However, *Btc* transgenic mice with additional loss of pancreatic ERBB4 are no longer protected against AP. Importantly, both cearulein and L-arginine pancreatitis models were used to exclude a caerulein-dependent effect. This finding ultimately confirms our presumption that ERBB4 mediates the protective effect of BTC.

4. Possible mechanisms mediating BTC-ERBB4 protection against AP

To learn more about the mechanisms underlying the ERBB4-mediated protection against AP, several signalling pathways such as SAPK, MAPK and AKT were investigated. ERBB receptors can also be processed from the cell surface by the action of secretases, definitely another interesting aspect as this relocalization might reveal an alternative signalling pathway (Linggi, 2006). On this way, ERBB4 may have the ability to influence the expression of several genes itself by acting as transcription factor (Kainulainen, 2000).

In previous studies, the protection of BTC could be demonstrated to be associated with an increased phosphorylation of SAPK (Dahlhoff, 2010). According to our Western blot analysis, phosphorylated SAPK is increased in the pancreas of *Btc* transgenic mice but not in the pancreas of *Btc* transgenic mice with additional deletion of ERBB4. These results suggest an activation of the SAPK pathway by BTC with an involvement of ERBB4. However, other main pathways of the ERBB receptors like MAPK or AKT could be involved in AP. Analysis of MAPK and AKT revealed no activation of these pathways by BTC. The MAPK pathway is activated in AP, probably due to its proinflammatory properties (Clemons, 2002), but obviously BTC is not involved in this signalling cascade. No alterations were found in AKT signalling, what differs to the findings in previous studies, where phosphorylated AKT is decreased during AP (Yang, 2011). This is a rather controversial result considering the established antiapoptotic properties of AKT (Li, 2015).

Because neither MAPK nor AKT signalling pathways are involved in the protection against AP by BTC, the endocytotic pathway of ERBB4 became even more interesting. It has already been reported that upon receptor activation the intracellular domain (ICD) of ERBB4 can be released in the cytoplasm and on this way might act as a transcription factor (Omerovic, 2004), (Lee, 2002), (Sundvall, 2008). The detection of ERBB4 in the different cell compartments revealed, as expected, a robust expression of ERBB4 in the membrane. Physiologically, the full length receptor may also be present in the cytoplasm and in the nucleus as a result of receptor internalization and degradation. In *Btc* transgenic mice, the detection of ERBB4 is increased in the nucleus. It cannot be excluded that even

the non-activated receptor could affect different intracellular processes and thereby influence the course of AP.

After activation of membrane bound ERBB4, a γ-secretase is able to cleave a 120 kDa ICD from the receptor, which can translocate to the nucleus. The increase of ICD in the cytoplasm and in the nucleus of *Btc* transgenic mice could be caused by the activation of ERBB4 by the overexpressed BTC, thus BTC could directly regulate the ICD amount in the cytoplasm. It can be assumed that the ICD acts as a transcriptional regulator as it has already been reported in several other tissues (Omerovic, 2004), (Lee, 2002), (Sundvall, 2008) and therefore might regulate the expression of different genes. In a further study it would be interesting to investigate the role of ICD in AP in more detail.

Against the background that ERBB4 may have the ability to influence gene expression indirectly and directly, we wanted to detect ERBB4 target genes which are relevant to the protection against AP. We investigated pancreas samples of *Btc* transgenic and wildtype mice with and without caerulein-induced AP in microarray analysis. The results of the microarray analysis revealed several genes which were upregulated by BTC signalling, including *Cbg* and *Pedf*. In previous studies, *Cbg* has been directly involved in the protection against AP (Muller, 2007). Other members of the Serpin-family, for instance *Spi2A*, have also been described to be involved in the protection against AP (Neuhofer, 2013) or such as *Pedf* in the development of pancreatic adenocarcinoma (Grippo, 2012). Upregulation of *Cbg* and *Pedf* in the pancreas of *Btc* transgenic mice suffering from AP was confirmed by qRT-PCR.

The increased expression of PEDF in *Btc* transgenic mice during AP could not be confirmed by Western blot analysis. Nevertheless, PEDF seems to play a role in AP in general, as it is increased in animals with AP. CBG, in contrast, is increased in the pancreas of *Btc* transgenic mice with and without AP. The physiological role of CBG is the transport of cortisol and its release in inflamed areas upon its cleavage by elastase (Hammond, 1990). In patients with a decreased CBG level within the initial 48 hours of AP, CBG was an early predictor of later infected pancreatic necrosis (Muller, 2007). Infected pancreatic necrosis is a serious complication that worsens prognosis in AP in human patients (Wronski, 2014). Endogenous cortisol might play a basic role in the course of AP and in the process of later infection (Muller, 2007). Thus, by increasing the levels of CBG in the

pancreas of transgenic mice, BTC may protect these mice against AP by promoting the anti-inflammatory effect of cortisol (Hammond, 1990).

To learn more about the role of CBG and cortisol in AP, it would be interesting to create and investigate mice with pancreas-specific overexpression of CBG. By employing the caerulein pancreatitis model it would be possible to figure out if these mice are protected against AP. Additionally, cortisol could be measured in the acinar cells of CBG-overexpressing mice with caerulein-induced pancreatitis to establish a relationship between CBG, cortisol and the protection against AP.

VI. ZUSAMMENFASSUNG

In dieser Arbeit wurde der protektive Effekt von BTC bei akuter Pankreatitis näher untersucht. In vorherigen Studien konnte nachgewiesen werden, dass Mäuse, die BTC ubiquitär überexprimieren vor akuter induzierter Pankreatitis geschützt sind. *Btc*-transgene Tiere zeigen außerdem ein signifikant reduziertes Pankreasgewicht, welches nicht über den EGF-Rezeptor vermittelt wird. Da der EGFR und der ERBB4-Rezeptor die einzigen Rezeptoren der ERBB-Familie sind, die durch BTC als Homodimere aktiviert werden können, wurden diese Rezeptoren in Mausmodellen untersucht, um die Rolle dieser Rezeptoren im exokrinen Pankreas und während der akuten Pankreatitis im Zusammenspiel mit ihrem Liganden BTC näher bestimmen zu können.

Zuerst konnte an einem EGFR-Knockdown-Mausmodell, mit zusätzlicher ubiquitären BTC-Überexprimierung, nachgewiesen werden, dass der protektive Effekt von BTC nicht EGFR vermittelt ist, da auch diese Tiere vor akuter Pankreatitis geschützt sind.

Mithilfe eines konditionalen ERBB4-Knockoutmodels konnte die Rolle von ERBB4 im exokrinen Pankreas untersucht werden und zudem, ob die Entwicklung der Maus durch den Verlust von ERBB4 im Pankreas beeinflusst wird. Der Verlust von ERBB4 im exokrinen Pankreas hatte keinen offensichtlichen Einfluss auf die Entwicklung der Maus oder auf das exokrine Pankreas. Auch der Verlauf der akuten induzierten Pankreatitis wurde nicht vom Verlust des ERBB4-Rezeptors beeinflusst. Jedoch konnte nach zusätzlicher BTC-Überexprimierung gezeigt werden, dass *Btc*-transgene Mäuse nicht mehr vor akuter Pankreatitis geschützt sind. Das zeigt, dass der protektive Effekt von BTC über ERBB4 vermittelt wird.

Um einen möglichen molekularbiologischen Mechansimus zu finden, der für den protektiven Effekt bei den *Btc*-transgenen Tieren verantwortlich ist, wurden verschiedene mögliche Signalkaskaden wie SAPK, MAPK und AKT näher untersucht. Der SAPK-Signalweg scheint durch die BTC-Überexpression verstärkt aktiviert zu werden. Außerdem konnte der ERBB4-Rezeptor selbst in verschiedenen Zellfraktionen des Pankreas nachgewiesen werden. Sowohl in der Membran als auch im Zytoplasma und im Zellkern konnte der Rezeptor detektiert

werden. Nach der Aktivierung von ERBB4 kann außerdem der zytoplasmatische Teil des ERBB4-Rezeptors, durch eine γ-Sekretase, abgespalten werden. Diese 120 kDa große Domäne des ERBB4-Rezeptors wurde verstärkt im Zytoplasma und zu einem geringen Anteil im Zellkern von *Btc*-transgenen Mäusen nachgewiesen. Aus der Literatur ist bekannt, dass die 120 kDa große intrazelluläre Domäne (ICD) in der Lage ist als Transkriptionsfaktor zu agieren. Durch die ICD kann die Expression verschiedener Gene direkt und indirekt beeinflusst werden.

Um mögliche Gene zu identifizieren, die protektiv in der Pankreatitis wirken, wurden Microarrays von Pankreasproben von *Btc*-transgenen Mäusen mit und ohne akuter Pankretitis durchgeführt. In den Microarrays wurde festgestellt, dass unter anderem *Cbg* während der akuten Pankreatitis bei *Btc*-transgenen Mäusen hochreguliert ist. Auch auf Proteinebene konnte eine stärkere Expression von CBG in Pankreas von *Btc*-transgenen Mäusen mit und ohne akuter Pankreatitis nachgewiesen werden. Das könnte auf eine mögliche Beteiligung von CBG am Schutz vor akuter Pankreatitis hinweisen. Ob die vermehrte Expression von CBG durch die Bindung von BTC an den ERBB4-Rezeptor ausgelöst wird, muss in weiteren Studien herausgefunden werden.

VII. SUMMARY

In this study the protective effect of BTC in AP was examined. Previous studies established that BTC protects mice against AP. Furthermore *Btc* transgenic mice show a significantly reduced pancreas weight, which is not mediated by the EGFR. Since EGFR and ERBB4 are the two homodimers which can be activated by BTC, different mouse models were examined in order to determine the role of the receptors in the exocrine pancreas and in AP in interaction with their ligand BTC.

In the EGFR knockdown model with an additional ubiquitous BTC-overexpression it could be confirmed that the protective effect of BTC is not mediated by EGFR, as these animals are still protected against induced AP.

The role of ERBB4 in the exocrine pancreas was investigated using a conditional ERBB4 knockout model. With this knockout model it was possible to figure out if the development of the mouse is influenced by the loss of ERBB4 in the exocrine pancreas. The loss of pancreatic ERBB4 did not affect the development of the mouse or the development of the exocrine pancreas. Even the course of AP was not modified by the loss of ERBB4. However, conditional ERBB4 knockout mice with additional BTC-overexpression, in contrast to *Btc* transgenic mice, are no longer protected against AP. Based on these findings it could be demonstrated that the protective effect caused by overexpressed BTC is ERBB4-dependent.

To find signal cascades which are triggered by the binding of BTC to the ERBB4 receptor, several pathways such as SAPK, MAPK and AKT were examined. It turned out that the SAPK pathway seems to be activated by this binding. In addition, the ERBB4 receptor itself could be detected in all examined cell fractions: the membrane, the cytoplasm and the nucleus. After activation the ERBB4 receptor can be cleaved and a 120 kDa domain (ICD) is released into the cytoplasm. This ICD showed an enhanced detection in the cytoplasm and a slight detection in the nucleus of mice overexpressing BTC. These results indicate that the 120 kDa domain of the ERBB4 receptor is known to act as transcription factor and thereby affect directly and indirectly the expression of different genes.

In order to detect these genes a microarray analysis was performed with pancreatic samples of *Btc* transgenic mice with and without AP. In the microarray

analysis, *Cbg* was detected to be upregulated in AP of *Btc* transgenic mice. CBG protein levels were also higher in the pancreas of *Btc* transgenic with and without pancreatitis, indicating an involvement of CBG in the protection against AP triggered by BTC. Further studies are needed to reveal whether the upregulation of CBG results from the activation of ERBB4 via BTC.

VIII. BIBLIOGRAPHY

Algul H, Wagner M, Lesina M, and Schmid RM (2007): Overexpression of ErbB2 in the exocrine pancreas induces an inflammatory response but not increased proliferation. International journal of cancer Journal international du cancer 121: 1410-1416.

Alimandi M, Wang LM, Bottaro D, Lee CC, Kuo A, Frankel M, Fedi P, Tang C, Lippman M, and Pierce JH (1997): Epidermal growth factor and BTC mediate signal transduction through co-expressed ErbB2 and ErbB3 receptors. The EMBO journal 16: 5608-5617.

Annemarie Thiel, (1953): Untersuchungen über das Gefässystem des Pankreasläppchens bei verschiedenen Säugern mit besonderer Berücksichtigung der Kapillarknäuel der Langerhansschen Inseln.

Barnard JA, Graves-Deal R, Pittelkow MR, DuBois R, Cook P, Ramsey GW, Bishop PR, Damstrup L, and Coffey RJ (1994): Auto- and cross-induction within the mammalian epidermal growth factor-related peptide family. The Journal of biological chemistry 269: 22817-22822.

Beerli RR, and Hynes NE (1996): Epidermal growth factor-related peptides activate distinct subsets of ErbB receptors and differ in their biological activities. The Journal of biological chemistry 271: 6071-6076.

Bramhall SR, Stamp GW, Dunn J, Lemoine NR, and Neoptolemos JP (1996): Expression of collagenase (MMP2), stromelysin (MMP3) and tissue inhibitor of the metalloproteinases (TIMP1) in pancreatic and ampullary disease. British journal of cancer 73: 972-978.

Clemons AP, Holstein DM, Galli A, and Saunders C (2002): Cerulein-induced AP in the rat is significantly ameliorated by treatment with MEK1/2 inhibitors U0126 and PD98059. Pancreas 25: 251-259.

Dahlhoff M, Algul H, Siveke JT, Lesina M, Wanke R, Wartmann T, Halangk W, Schmid RM, Wolf E, and Schneider MR (2010): BTC protects from pancreatitis by activating stress-activated protein kinase. Gastroenterology 138: 1585-1594, 1594 e1581-1583.

Delaspre F, Massumi M, Salido M, Soria B, Ravassard P, Savatier P, and Skoudy A (2013): Directed pancreatic acinar differentiation of mouse embryonic stem cells via embryonic signalling molecules and exocrine transcription factors. PloS one 8: e54243.

Dembinski A, Gregory H, Konturek SJ, and Polanski M (1982): Trophic action of epidermal growth factor on the pancreas and gastroduodenal mucosa in rats. The Journal of physiology 325: 35-42.

Dunbar AJ, and Goddard C (2000): Structure-function and biological role of BTC. The international journal of biochemistry & cell biology 32: 805-815.

Elenius K, Choi CJ, Paul S, Santiestevan E, Nishi E, and Klagsbrun M (1999): Characterization of a naturally occurring ErbB4 isoform that does not bind or activate phosphatidyl inositol 3-kinase. Oncogene 18: 2607-2615.

Frey MR, Edelblum KL, Mullane MT, Liang D, and Polk DB (2009): The ErbB4 growth factor receptor is required for colon epithelial cell survival in the presence of TNF. Gastroenterology 136: 217-226.

Gassmann M, Casagranda F, Orioli D, Simon H, Lai C, Klein R, and Lemke G (1995): Aberrant neural and cardiac development in mice lacking the ErbB4 neuregulin receptor. Nature 378: 390-394.

Golstein P, and Kroemer G (2007): Cell death by necrosis: towards a molecular definition. Trends in biochemical sciences 32: 37-43.

Gomez-Gaviro MV, Scott CE, Sesay AK, Matheu A, Booth S, Galichet C, and Lovell-Badge R (2012): BTC promotes cell proliferation in the neural stem cell niche and stimulates neurogenesis. Proceedings of the National Academy of Sciences of the United States of America 109: 1317-1322.

Grippo PJ, Fitchev PS, Bentrem DJ, Melstrom LG, Dangi-Garimella S, Krantz SB, Heiferman MJ, Chung C, Adrian K, Cornwell ML, Flesche JB, Rao SM, Talamonti MS, Munshi HG, and Crawford SE (2012): Concurrent PEDF deficiency and Kras mutation induce invasive pancreatic cancer and adipose-rich stroma in mice. Gut 61: 1454-1464.

Gukovskaya AS, and Pandol SJ (2004): Cell death pathways in pancreatitis and pancreatic cancer. Pancreatology : official journal of the International Association of Pancreatology 4: 567-586.

Hammond GL, Smith CL, Paterson NA, and Sibbald WJ (1990): A role for corticosteroid-binding globulin in delivery of cortisol to activated neutrophils. The Journal of clinical endocrinology and metabolism 71: 34-39.

Harris RC, Chung E, and Coffey RJ (2003): EGF receptor ligands. Experimental cell research 284: 2-13.

Holbro T, Civenni G, and Hynes NE (2003): The ErbB receptors and their role in cancer progression. Experimental cell research 284: 99-110.

Huotari MA, Miettinen PJ, Palgi J, Koivisto T, Ustinov J, Harari D, Yarden Y, and Otonkoski T (2002): ErbB signaling regulates lineage determination of developing pancreatic islet cells in embryonic organ culture. Endocrinology 143: 4437-4446.

Jackson LF, Qiu TH, Sunnarborg SW, Chang A, Zhang C, Patterson C, and Lee DC (2003): Defective valvulogenesis in HB-EGF and TACE-null mice is associated with aberrant BMP signaling. The EMBO journal 22: 2704-2716.

Jones FE, Golding JP, and Gassmann M (2003): ErbB4 signaling during breast and neural development: novel genetic models reveal unique ErbB4 activities. Cell cycle 2: 555-559.

Kainulainen V, Sundvall M, Maatta JA, Santiestevan E, Klagsbrun M, and Elenius K (2000): A natural ErbB4 isoform that does not activate phosphoinositide 3-kinase mediates proliferation but not survival or chemotaxis. The Journal of biological chemistry 275: 8641-8649.

Kawaguchi J, Wilson V, and Mee PJ (2002): Visualization of whole-mount skeletal expression patterns of LacZ reporters using a tissue clearing protocol. BioTechniques 32: 66, 68-70, 72-63.

Kawaguchi M, Hosotani R, Kogire M, Ida J, Doi R, Koshiba T, Miyamoto Y, Tsuji S, Nakajima S, Kobayashi H, Masui T, and Imamura M (2000): Auto-induction and growth stimulatory effect of BTC in human pancreatic cancer cells. International journal of oncology 16: 37-41.

Konturek SJ, Cieszkowski M, Jaworek J, Konturek J, Brzozowski T, and Gregory H (1984): Effects of epidermal growth factor on gastrointestinal secretions. The American journal of physiology 246: G580-586.

Kritzik MR, Krahl T, Good A, Gu D, Lai C, Fox H, and Sarvetnick N (2000): Expression of ErbB receptors during pancreatic islet development and regrowth. The Journal of endocrinology 165: 67-77.

Lazarow A (1957): Cell types of the islets of Langerhans and the hormones they produce. Diabetes 6: 222-232; discussion, 232-223.

Lee D, Cross SH, Strunk KE, Morgan JE, Bailey CL, Jackson IJ, and Threadgill DW (2004): Wa5 is a novel ENU-induced antimorphic allele of the epidermal growth factor receptor. Mammalian genome : official journal of the International Mammalian Genome Society 15: 525-536.

Lee HJ, Jung KM, Huang YZ, Bennett LB, Lee JS, Mei L, and Kim TW (2002): Presenilin-dependent gamma-secretase-like intramembrane cleavage of ErbB4. The Journal of biological chemistry 277: 6318-6323.

Li B, Wang Z, Zhong Y, Lan J, Li X, and Lin H (2015): CCR9-CCL25 interaction suppresses apoptosis of lung cancer cells by activating the PI3K/Akt pathway. Medical oncology 32: 531.

Li L, Seno M, Yamada H, and Kojima I (2001): Promotion of beta-cell regeneration by BTC in ninety percent-pancreatectomized rats. Endocrinology 142: 5379-5385.

Linggi B, and Carpenter G (2006): ErbB receptors: new insights on mechanisms and biology. Trends in cell biology 16: 649-656.

Luetteke NC, Qiu TH, Fenton SE, Troyer KL, Riedel RF, Chang A, and Lee DC (1999): Targeted inactivation of the EGF and amphiregulin genes reveals distinct roles for EGF receptor ligands in mouse mammary gland development. Development 126: 2739-2750.

Luetteke NC, Qiu TH, Peiffer RL, Oliver P, Smithies O, and Lee DC (1993): TGF alpha deficiency results in hair follicle and eye abnormalities in targeted and waved-1 mice. Cell 73: 263-278.

Manto MU, and Jissendi P (2012): Cerebellum: links between development, developmental disorders and motor learning. Frontiers in neuroanatomy 6: 1.

Massague J, and Pandiella A (1993): Membrane-anchored growth factors. Annual review of biochemistry 62: 515-541.

Matsumoto K, Miyake Y, Nakatsu M, Toyokawa T, Ando M, Hirohata M, Kato H, and Yamamoto K (2014): Usefulness of Early-phase Peritoneal Lavage for Treating Severe AP. Internal medicine 53: 1-6.

Matull WR, Pereira SP, and O'Donohue JW (2006): Biochemical markers of AP. Journal of clinical pathology 59: 340-344.

Muller CA, Belyaev O, Vogeser M, Weyhe D, Gloor B, Strobel O, Werner J, Borgstrom A, Buchler MW, Uhl W (2007): Corticosteroid-binding globulin: a possible early predictor of infection in acute necrotizing pancreatitis. Scandinavian journal of gastroenterology 42: 1354-1361

Nair G, Vincent RK, and Odorico JS (2013): Ectopic Ptf1a expression in murine ESCs potentiates endocrine differentiation and models pancreas development in vitro. Stem cells.

Naresh A, Long W, Vidal GA, Wimley WC, Marrero L, Sartor CI, Tovey S, Cooke TG, Bartlett JM, and Jones FE (2006): The ERBB4/HER4 intracellular domain 4ICD is a BH3-only protein promoting apoptosis of breast cancer cells. Cancer research 66: 6412-6420.

Nemeth BC, Wartmann T, Halangk W, and Sahin-Toth M (2013): Autoactivation of mouse trypsinogens is regulated by chymotrypsin C via cleavage of the autolysis loop. The Journal of biological chemistry 288: 24049-24062.

Neuhofer P, Liang S, Einwachter H, Schwerdtfeger C, Wartmann T, Treiber M, Zhang H, Schulz HU, Dlubatz K, Lesina M, Diakopoulos KN, Wormann S, Halangk W, Witt H, Schmid RM, and Algul H (2013): Deletion of IkappaBalpha activates RelA to reduce AP in mice through up-regulation of Spi2A. Gastroenterology 144: 192-201.

Niederau C, Ferrell LD, and Grendell JH (1985): Caerulein-induced acute necrotizing pancreatitis in mice: protective effects of proglumide, benzotript, and secretin. Gastroenterology 88: 1192-1204.

Ogata T, Dunbar AJ, Yamamoto Y, Tanaka Y, Seno M, and Kojima I (2005): BTC-delta4, a novel differentiation factor for pancreatic beta-cells, ameliorates glucose intolerance in streptozotocin-treated rats. Endocrinology 146: 4673-4681.

Olayioye MA, Neve RM, Lane HA, and Hynes NE (2000): The ErbB signaling network: receptor heterodimerization in development and cancer. The EMBO journal 19: 3159-3167.

Omerovic J, Puggioni EM, Napoletano S, Visco V, Fraioli R, Frati L, Gulino A, and Alimandi M (2004): Ligand-regulated association of ErbB-4 to the transcriptional co-activator YAP65 controls transcription at the nuclear level. Experimental cell research 294: 469-479.

P OC, Rhys-Evans P, and Eccles S (2000): Expression and regulation of c-ERBB ligands in human head and neck squamous carcinoma cells. International journal of cancer Journal international du cancer 88: 759-765.

Pinkas-Kramarski R, Lenferink AE, Bacus SS, Lyass L, van de Poll ML, Klapper LN, Tzahar E, Sela M, van Zoelen EJ, and Yarden Y (1998): The oncogenic ErbB-2/ErbB-3 heterodimer is a surrogate receptor of the epidermal growth factor and BTC. Oncogene 16: 1249-1258.

Plowman GD, Culouscou JM, Whitney GS, Green JM, Carlton GW, Foy L, Neubauer MG, and Shoyab M (1993): Ligand-specific activation of HER4/p180erbB4, a fourth member of the epidermal growth factor receptor family. Proceedings of the National Academy of Sciences of the United States of America 90: 1746-1750.

Purevdorj E, Zscheppang K, Hoymann HG, Braun A, von Mayersbach D, Brinkhaus MJ, Schmiedl A, and Dammann CE (2008): ErbB4 deletion leads to changes in lung function and structure similar to bronchopulmonary dysplasia. American journal of physiology Lung cellular and molecular physiology 294: L516-522.

Qin L, Tamasi J, Raggatt L, Li X, Feyen JH, Lee DC, Dicicco-Bloom E, and Partridge NC (2005): Amphiregulin is a novel growth factor involved in normal bone development and in the cellular response to parathyroid hormone stimulation. The Journal of biological chemistry 280: 3974-3981.

Rio C, Buxbaum JD, Peschon JJ, and Corfas G (2000): Tumor necrosis factor-alpha-converting enzyme is required for cleavage of erbB4/HER4. The Journal of biological chemistry 275: 10379-10387.

Rubio F, Gassmann W, and Schroeder JI (1995): Sodium-driven potassium uptake by the plant potassium transporter HKT1 and mutations conferring salt tolerance. Science (New York, NY) 270: 1660-1663.

Ryu JY, Siswanto A, Harimoto K, and Tagawa Y (2013): Chimeric analysis of EGFP and DsRed2 transgenic mice demonstrates polyclonal maintenance of pancreatic acini. Transgenic research 22: 549-556.

Sahin U, Weskamp G, Kelly K, Zhou HM, Higashiyama S, Peschon J, Hartmann D, Saftig P, and Blobel CP (2004): Distinct roles for ADAM10 and ADAM17 in ectodomain shedding of six EGFR ligands. The Journal of cell biology 164: 769-779.

Sartor CI, Zhou H, Kozlowska E, Guttridge K, Kawata E, Caskey L, Harrelson J, Hynes N, Ethier S, Calvo B, and Earp HS, 3rd (2001): Her4 mediates ligand-dependent antiproliferative and differentiation responses in human breast cancer cells. Molecular and cellular biology 21: 4265-4275.

Scheller J, Chalaris A, Garbers C, and Rose-John S (2011): ADAM17: a molecular switch to control inflammation and tissue regeneration. Trends in immunology 32: 380-387.

Schepers NJ, Besselink MG, van Santvoort HC, Bakker OJ, Bruno MJ, and Dutch Pancreatitis Study G (2013): Early management of AP. Best practice & research Clinical gastroenterology 27: 727-743.

Schmid RM (2005): Pathophysiology of AP. If you believe in mice--it's time for conditional gene targeting! Digestion 71: 159-161.

Schneider MR, Dahlhoff M, Herbach N, Renner-Mueller I, Dalke C, Puk O, Graw J, Wanke R, and Wolf E (2005): BTC overexpression in transgenic mice causes disproportionate growth, pulmonary hemorrhage syndrome, and complex eye pathology. Endocrinology 146: 5237-5246.

Schneider MR, and Wolf E (2009): The epidermal growth factor receptor ligands at a glance. Journal of cellular physiology 218: 460-466.

Shing Y, Christofori G, Hanahan D, Ono Y, Sasada R, Igarashi K, and Folkman J (1993): BTC: a mitogen from pancreatic beta cell tumors. Science (New York, NY) 259: 1604-1607.

Shirakata Y, Tokumaru S, Sayama K, and Hashimoto K (2010): Auto- and cross-induction by BTC in epidermal keratinocytes. Journal of dermatological science 58: 162-164.

Shirasawa S, Sugiyama S, Baba I, Inokuchi J, Sekine S, Ogino K, Kawamura Y, Dohi T, Fujimoto M, and Sasazuki T (2004): Dermatitis due to epiregulin deficiency and a critical role of epiregulin in immune-related responses of keratinocyte and macrophage. Proceedings of the National Academy of Sciences of the United States of America 101: 13921-13926.

Srinivasan R, Poulsom R, Hurst HC, and Gullick WJ (1998): Expression of the c-erbB-4/HER4 protein and mRNA in normal human fetal and adult tissues and in a survey of nine solid tumour types. The Journal of pathology 185: 236-245.

Soriano P. (1999): Generalized lacZ expression with the ROSA26 Cre reporter strain. Nature Genetics 21: 1061-4036

Stephen J. Pandol: The exocrine pancreas, ebook ISBN 9781615041398 .S.3-8

Sundvall M, Korhonen A, Paatero I, Gaudio E, Melino G, Croce CM, Aqeilan RI, and Elenius K (2008): Isoform-specific monoubiquitination, endocytosis, and degradation of alternatively spliced ErbB4 isoforms. Proceedings of the National Academy of Sciences of the United States of America 105: 4162-4167.

Sweeney C, and Carraway KL, 3rd (2000): Ligand discrimination by ErbB receptors: differential signaling through differential phosphorylation site usage. Oncogene 19: 5568-5573.

te Velde EA, Franke AC, van Hillegersberg R, Elshof SM, de Weger RW, Borel Rinkes IH, and van Diest PJ (2009): HER-family gene amplification and expression in resected pancreatic cancer. European journal of surgical oncology : the journal of the European Society of Surgical Oncology and the British Association of Surgical Oncology 35: 1098-1104.

Tylor Stevens (2009): AP: Problems in adherence to guidelines. Cleveland Clinic Journal of Medicine**:** 697-704.

Veikkolainen V, Naillat F, Railo A, Chi L, Manninen A, Hohenstein P, Hastie N, Vainio S, and Elenius K (2012): ErbB4 modulates tubular cell polarity and lumen diameter during kidney development. Journal of the American Society of Nephrology : JASN 23: 112-122.

Vidal GA, Naresh A, Marrero L, and Jones FE (2005): Presenilin-dependent gamma-secretase processing regulates multiple ERBB4/HER4 activities. The Journal of biological chemistry 280: 19777-19783.

Vonlaufen A, Wilson JS, Pirola RC, and Apte MV (2007): Role of alcohol metabolism in chronic pancreatitis. Alcohol research & health: the journal of the National Institute on Alcohol Abuse and Alcoholism 30: 48-54.

Westlund KN (2009): Gene therapy for pancreatitis pain. Gene therapy 16: 483-492.

Wronski M, Cebulski W, Slodkowski M, Krasnodebski IW (2014): Minimally invasive treatment of infected pancreatic necrosis. Przeglad gastroenterologiczny 9: 317-324

Yang SJ, Chen HM, Hsieh CH, Hsu JT, Yeh CN, Yeh TS, Hwang TL, Jan YY, and Chen MF (2011): Akt pathway is required for oestrogen-mediated attenuation of lung injury in a rodent model of cerulein-induced AP. Injury 42: 638-642.

Yarden Y, and Sliwkowski MX (2001): Untangling the ErbB signalling network. Nature reviews Molecular cell biology 2: 127-137.

Yokoyama M, Funatomi H, Kobrin M, Ebert M, Friess H, Buchler M, and Korc M (1995): BTC, a member of the epidermal growth-factor family, is overexpressed in human pancreatic-cancer. International journal of oncology 7: 825-829.

Zeng F, Xu J, and Harris RC (2009): Nedd4 mediates ErbB4 JM-a/CYT-1 ICD ubiquitination and degradation in MDCK II cells. FASEB journal : official publication of the Federation of American Societies for Experimental Biology 23: 1935-1948

IX. ACKNOWLEDGEMENT

First of all, I would like to thank with a deep sense of gratitude Dr. Maik Dahlhoff for his constant support, encouragement and individual guidance through my research. My special appreciation goes to PD Dr. Marlon R. Schneider for his support and for his helpful annotations. I want to thank also PD Dr. Hana Algül (Klinkum rechts der Isar) for the pleasant collaboration and especially for his time and discussing scientific problems always in a kind manner. I am indebted to Prof. Dr. Eckhard Wolf for allowing me to carry out my research at the Institute for Molecular Animal Breeding and Biotechnology, Gene Center, and for the excellent working conditions.

I am particularly grateful to Stefanie Riesemann, Sepp Millauer, Kathrin Hedegger and Freya Jay for their consistent help and friendship, especially during my pregnancy. My special thank goes also to Dr. Ingrid Renner-Müller, Petra Renner, Insa Härtel and all the present and former members of the animal maintenance crew for the excellent management of the mice strains and their constant help and advice with laboratory animal care. Furthermore I especially want to thank Sylvia Hornig for the provided workplace and great atmosphere and Tamara Holy, Felix Hiltwein, Mai Johanna Le, Sabrina Porada and Jessica Grill for the good time we had in the lab together. Not forgetting the girls in the histolab (Veterinärpathologie, LMU), who have helped me with the sections always in combination with a nice conversation.

Finally my special thanks go to my family, especially to my husband for his support and patience but also to my parents and my mother-in-law for their baby-sitting services. Without you writing this thesis would not have been possible.